

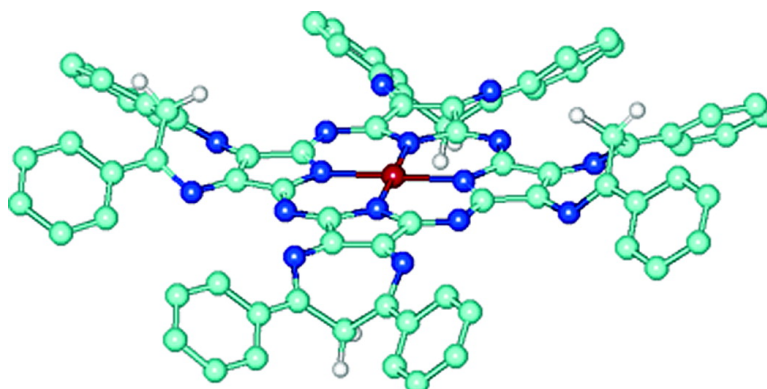
Article

Porphyrazines with Annulated Diazepine Rings. 2. Alternative Synthetic Route to Tetrakis-2,3-(5,7-diphenyl-1,4-diazepino)porphyrazines: New Metal Complexes, General Physicochemical Data, Ultraviolet–Visible Linear and Optical Limiting Behavior, and Electrochemical and Spectroelectrochemical Properties

Maria Pia Donzello, Danilo Dini, Giuseppe D'Arcangelo, Claudio Ercolani, Riqiang Zhan, Zhongping Ou, Pavel A. Stuzhin, and Karl M. Kadish

J. Am. Chem. Soc., **2003**, 125 (46), 14190-14204 • DOI: 10.1021/ja0344361 • Publication Date (Web): 23 October 2003

Downloaded from <http://pubs.acs.org> on March 30, 2009



More About This Article

Additional resources and features associated with this article are available within the HTML version:

- Supporting Information
- Links to the 8 articles that cite this article, as of the time of this article download
- Access to high resolution figures
- Links to articles and content related to this article
- Copyright permission to reproduce figures and/or text from this article

[View the Full Text HTML](#)



ACS Publications
High quality. High impact.

Porphyrazines with Annulated Diazepine Rings. 2. Alternative Synthetic Route to Tetrakis-2,3-(5,7-diphenyl-1,4-diazepino)porphyrazines: New Metal Complexes, General Physicochemical Data, Ultraviolet–Visible Linear and Optical Limiting Behavior, and Electrochemical and Spectroelectrochemical Properties

Maria Pia Donzello,[†] Danilo Dini,[‡] Giuseppe D'Arcangelo,[§] Claudio Ercolani,^{*,†} Riqiang Zhan,^{||} Zhongping Ou,^{||} Pavel A. Stuzhin,^{*,⊥} and Karl M. Kadish^{*,||}

Contribution from the Dipartimento di Chimica, Università degli Studi di Roma "La Sapienza", P.le A. Moro 5, Roma, I-00185, Italy, Institut für Organische Chemie, Universität Tübingen, D-72076 Tübingen, Germany, Dipartimento di Scienze e Tecnologie Chimiche, Università di Tor Vergata, via della Ricerca Scientifica, Roma, I-00133, Italy, Department of Chemistry, University of Houston, Houston, Texas 77204-5003, and Department of Organic Chemistry, Ivanovo State University of Chemical Technology, Friedrich Engels Pr-t 7, Ivanovo, RF-153460, Russia

Received January 31, 2003; E-mail: claudio.ercolani@uniroma1.it

Abstract: Following a previous report on the synthesis and physicochemical characterization of a novel class of porphyrazines carrying peripherally annulated seven-membered rings, i.e., tetrakis-2,3-(5,7-diphenyl-1,4-diazepino)porphyrazine [Ph₈DzPzH₂] \cdot 4H₂O and its metal derivatives [Ph₈DzPzM] \cdot xH₂O (x = 2–7, M = Mg^{II}(H₂O), Cu^{II}, and Zn^{II}), a new more convenient procedure is reported here, allowing the preparation in high yields of the Li^I and Na^I derivatives of formulas [Ph₈DzPzLi₂] \cdot 5H₂O and [Ph₈DzPzNa₂] \cdot 6H₂O, which can be directly converted into other metal derivatives under mild conditions (room temperature) and in good yields. The series studied has been extended to include the Mn^{II} and Co^{II} complexes also reported here for the first time. Physicochemical characterization of the new "diazepinoporphyrazines" was based on fast atom bombardment (FAB) mass spectrometry and X-ray powder patterns, infrared (IR), electron paramagnetic resonance (EPR), and room-temperature magnetic susceptibility measurements. A detailed discussion of the UV–vis spectra emphasizes the role played by the external diazepine rings in electron delocalization through their tautomeric or protonated forms present in neutral, basic, and acidic media. The nonlinear optical effect of optical limiting for the different species [M = 2H, Mg^{II}(H₂O), Mn^{II}, Co^{II}, Cu^{II}, and Zn^{II}] has also been measured. It has been observed that the extent of the optical limiting depends on the specific M center. The observed nonlinear optical features are analyzed and discussed in terms of the electronic and magnetic properties exhibited by some of the metal ions and taking into account the model of the excited-state absorption in which the nature of M determines the kinetics of formation of the highly absorbing state of the specific complex examined. As evidenced by the detailed electrochemical and spectroelectrochemical study carried out on this new class of macrocycles, one of the most important aspects is the facilitated electron delocalization for the oxidized and reduced species allowed by a 1H–6H tautomerism taking place on the peripheral diazepine rings.

Introduction

Porphyrazines, unlike the related much-examined phthalocyanines,^{1,2} have until recently received little attention in the literature, but they are now the subject of increasing importance

and interest as to their synthesis, properties, and applications.^{3,4} In the course of our studies on such tetrapyrrolic macrocycles, we have investigated the synthesis and physicochemical properties of new porphyrazine macrocycles having peripheral heterocyclic five-,⁵ six-,⁶ and seven-membered rings.⁷ Part of this work reported on a class of porphyrazine derivatives containing external annulated heptaatomic diazepine rings, i.e., solvated tetrakis-2,3-(5,7-diphenyl-1,4-diazepino)porphyrazine, [Ph₈-

[†] Università degli Studi di Roma "La Sapienza".

[‡] Universität Tübingen.

[§] Università di Tor Vergata.

^{||} University of Houston.

[⊥] Ivanovo State University of Chemical Technology.

(1) *Phthalocyanines: Properties and Applications*; Leznoff, C. C., Lever, A. B. P., Eds.; VCH Publishers: New York, 1989–1996; Vols. 1–4.

(2) *The Porphyrin Handbook*; Kadish, K. M., Smith, K. M., Guillard, R., Eds.; Academic Press: New York, 2003; Vols. 17 and 19.

(3) Stuzhin, P. A.; Ercolani, C. In *The Porphyrin Handbook*; Kadish, K. M., Smith, K. M., Guillard, R., Eds.; Academic Press: New York, 2003; Vol. 15, Chapt. 101, pp 263–364.

(4) Michel, S. L. J.; Hoffman, B. M.; Baum, S. M.; Barrett, A. G. M. *Prog. Inorg. Chem.* **2001**, *50*, 473.

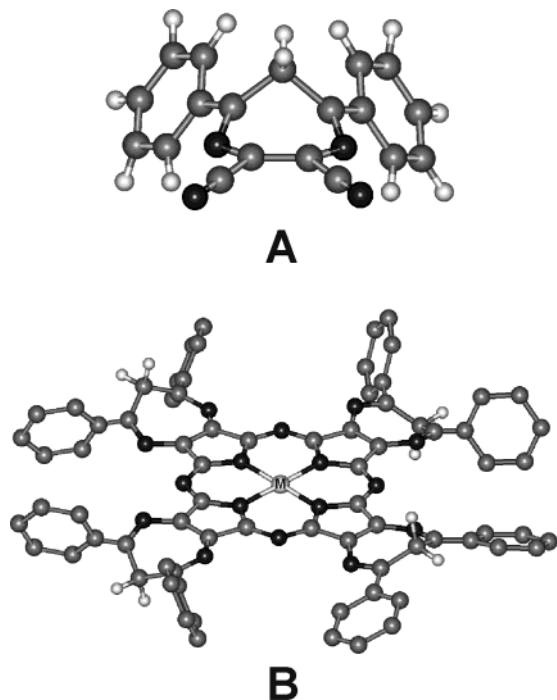


Figure 1. (A) Front-top view of $\text{Ph}_2\text{Dz}(\text{CN})_2$ (X-ray data in ref 7) and (B) computer-generated molecular model (MM+ force field) of a “diazepinoporphyrazine” complex $[\text{Ph}_8\text{DzPzM}]$ (hydrogen atoms of phenyl groups are omitted for clarity).

DzPzH_2 ·4 H_2O , and its corresponding complexes of formula $[\text{Ph}_8\text{DzPzM}] \cdot x\text{H}_2\text{O}$ [$\text{M} = \text{Mg}^{\text{II}}(\text{H}_2\text{O}), \text{Cu}^{\text{II}}, \text{Zn}^{\text{II}}; x = 2-7$], obtained by using as a precursor 5,7-diphenyl-2,3-dicyano-1,4-diazepine, $\text{Ph}_2\text{Dz}(\text{CN})_2$ (Figure 1A).⁷

To our knowledge,³ this new class of symmetrical porphyrazine macrocycles bearing peripherally annulated seven-membered heterocyclic rings has so far no counterpart in the literature. Based on available structural data on $\text{Ph}_2\text{Dz}(\text{CN})_2$ ⁷ and extensive information from NMR data on the related Zn^{II} and Mg^{II} complexes,⁷ a computer-generated representation of the molecular structure of an unsolvated species $[\text{Ph}_8\text{DzPzM}]$ is given in Figure 1B.

There are potentially a number of practical applications for macrocyclic porphyrazine materials. This is particularly the case for the related phthalocyanine macrocycles^{1,2} and interesting aspects may also pertain to the present “diazepinoporphyrazine” complexes in view of their combined chromophoric properties and solubility. In light of this, work on this class of materials has been further extended from our initial study,⁷ and we report here on the synthesis and characterization of new $\text{Li}^{\text{I}}, \text{Na}^{\text{I}}, \text{Mn}^{\text{II}},$ and Co^{II} derivatives. We also show that the lithium and sodium complexes, having the formula $[\text{Ph}_8\text{DzPzM}] \cdot x\text{H}_2\text{O}$ ($\text{M} = \text{Li}_2$ and $\text{Na}_2; x = 5-6$), open up a new quite convenient route for the preparation of several other metal complexes, thus providing an alternative synthetic methodology to the procedure that uses

the free-base ligand $[\text{Ph}_8\text{DzPzH}_2] \cdot 4\text{H}_2\text{O}$ after demetalation of the corresponding Mg^{II} complex.⁷ The physicochemical characterization of each $[\text{Ph}_8\text{DzPzM}] \cdot x\text{H}_2\text{O}$ ($x = 4-9$) species presented in this paper is based on fast atom bombardment (FAB) mass spectrometry and thermogravimetric analysis, X-ray powder diffraction, IR and electron paramagnetic resonance (EPR) spectra, and room-temperature magnetic susceptibility measurements. The UV-vis spectral behavior of each compound has also been studied in detail, with the work further extended to the nonlinear optical properties, namely, optical limiting, by using the Z-scan technique, not considered before for these compounds;⁷ this is in view of the fact that tetrapyrrolic systems such as porphyrazines, and especially phthalocyanines and porphyrins, are π -electron conjugated macrocycles able to give rise to a nonlinear optical (NLO) effect of optical limiting (OL)⁸ via a mechanism based upon the excited-state absorption operating in the UV-vis-near IR wavelength range.⁹ As known, the OL effect consists of the transmission of a constant flux of photons through a material or a device once the intensity of the incident radiation exceeds a system-characteristic threshold of intensity.¹⁰⁻¹³

Finally, the electrochemical and spectroelectrochemical behavior of the present species have also been explored in order to examine the involvement of the metal centers and the role played by the central porphyrazine site and/or the peripheral diazepine rings in charge localization or redistribution after the observed redox processes. This information can also be of importance for future electrochemical and electrochromic investigations on thin solid films of this new series of macrocyclic materials.

Experimental Section

Solvents and Chemicals. Solvents ($\text{CH}_3\text{OH}, \text{CH}_2\text{Cl}_2, \text{CHCl}_3, \text{CH}_3\text{-CN}, \text{CH}_3\text{COCH}_3, \text{benzene}, \text{hexane}, 96\% \text{H}_2\text{SO}_4, \text{HCl}, \text{CH}_3\text{COOH},$ and acetic anhydride) and reagents [$\text{CaH}_2, \text{Na},$ and Li metals, and hydrated $\text{Mn}^{\text{II}}, \text{Co}^{\text{II}}, \text{Zn}^{\text{II}},$ and Cu^{II} acetates] were purchased as high-purity chemicals and used as received (Carlo Erba, Aldrich, Merck). Pyridine and dimethyl sulfoxide (DMSO) were freshly distilled before use over CaH_2 . Ethyl and amyl alcohols were made anhydrous by distillation over Na.

New synthetic procedures, described below, were developed for preparation of the lithium and sodium derivatives, i.e., $[\text{Ph}_8\text{DzPzLi}_2] \cdot 5\text{H}_2\text{O}$ and $[\text{Ph}_8\text{DzPzNa}_2] \cdot 6\text{H}_2\text{O}$ and, from the latter species, for the free-base macrocycle and its $\text{Co}^{\text{II}}, \text{Cu}^{\text{II}},$ and Zn^{II} complexes.

Tetrakis-2,3-(5,7-diphenyl-1,4-diazepino)porphyrinatodisodium(I) Hexahydrate, $[\text{Ph}_8\text{DzPzNa}_2] \cdot 6\text{H}_2\text{O}$. Sodium metal (200 mg, 8.7 mmol) was suspended in freshly distilled ethyl alcohol (20 mL), in an inert atmosphere with stirring. The suspension was heated for a few minutes to determine the complete conversion of Na into its corresponding ethanolate. $\text{Ph}_2\text{Dz}(\text{CN})_2$ (5.2 g, 17.4 mmol) was then added and the mixture kept refluxing for 40 min. The yellow mixture changed to dark green during the reaction and then to dark blue. At the end of the reaction, the blue powder was separated by filtration, washed with methanol, and brought to constant weight under vacuum. Yield: 4.77 g (82%). Calcd. for $[\text{Ph}_8\text{DzPzNa}_2] \cdot 6\text{H}_2\text{O}, \text{C}_{76}\text{H}_{60}\text{N}_2\text{Na}_2\text{O}_6$ (MW 1339.40): C, 68.15; H, 4.51; N, 16.73. Found: C, 68.36; H, 4.51; N, 16.14. TGA showed a weight loss of 7.2% (calcd for six molecules of

(5) (a) Stuzhin, P. A.; Bauer, E. M.; Ercolani, C. *Inorg. Chem.* **1998**, *37*, 1533. (b) Bauer, E. M.; Cardarilli, D.; Ercolani, C.; Stuzhin, P. A.; Russo, U. *Inorg. Chem.* **1999**, *38*, 6114. (c) Bauer, E. M.; Ercolani, C.; Galli, P.; Popkova, I. A.; Stuzhin, P. A. *J. Porphyrins Phthalocyanines* **1999**, *3*, 371. (d) Angeloni, S.; Bauer, E. M.; Ercolani, C.; Popkova, I. A.; Stuzhin, P. A. *J. Porphyrins Phthalocyanines* **2001**, *5*, 881.
(6) Reference 1c and unpublished results.
(7) Donzello, M. P.; Ercolani, C.; Stuzhin, P. A.; Chiesi-Villa, A.; Rizzoli, C. *Eur. J. Inorg. Chem.* **1999**, 2075. In this cited paper, on page 2077, right column, line 16, “in dimethyl sulfoxide (DMSO)” should be substituted by “in pyridine”.

(8) Sheik-Bahae, M.; Said, A.; Wei, T.; Hagan, D. J.; Van Stryland, E. W. *IEEE J. Quantum Electron.* **1990**, *26*, 760.
(9) Hercher, M. *Appl. Opt.* **1967**, *6*, 947.
(10) Gires, F. *IEEE J. Quantum Electron.* **1966**, *QE-2*, 624.
(11) Tutt, L. W.; Boggess, T. F. *Prog. Quantum Electron.* **1993**, *17*, 299.
(12) Sun, Y. P.; Riggs, J. E. *Int. Rev. Phys. Chem.* **1999**, *18*, 43.
(13) Dini, D.; Barthel, M.; Hanack, M. *Eur. J. Org. Chem.* **2001**, 3759.

water, 8.1%). MS (liquid mass), m/z : 1232.5 $[M - 6H_2O]^+$. UV-vis (pyridine): λ_{\max} ($\lg \epsilon$) = 359 (4.84), 643 (4.62), 688 (4.42). IR (cm^{-1}): 1650 w, 1625 w, 1600 vw, 1525 s, 1498 w, 1445 s, 1385 s, 1319 m, 1305 sh, 1272 s, 1125 sh, 1165 s, 1120 s, 1075 w, 1042 s, 1025 m, 1002 w, 980 m, 950 w, 925 vw, 845 vw, 770 (sh), 755 vs, 695 vs, 655 vw, 615 vw, 602 vw, 420 vw. The sodium salt shows good solubility in common solvents such as ethanol, methanol, acetonitrile, acetone ($\approx 10^{-3}$ mol/L), or benzene ($\approx 10^{-4}$ mol/L) and insolubility in hexane.

Tetrakis-2,3-(5,7-diphenyl-1,4-diazepino)porphyrinatodilithium(I) Pentahydrate, $[Ph_8DzPzLi_2] \cdot 5H_2O$. Lithium metal (40 mg, 5.8 mmol) was suspended in an inert atmosphere, with stirring, in freshly distilled amyl alcohol (20 mL). The suspension was heated for 2 h to determine the complete conversion of Li into its corresponding amylate. $Ph_2Dz(CN)_2$ (3.60 g, 12.1 mmol) was then added, and the mixture kept refluxing for 40 min. The yellow mixture changed to dark green during the reaction and then to dark blue. At the end of the reaction, the bluish solid was separated by filtration, washed with methanol, and brought to constant weight under vacuum. Yield: 2.96 g (76%). Calcd for $[Ph_8DzPzLi_2] \cdot 5H_2O$, $C_{76}H_{58}Li_2N_{16}O_5$ (MW 1289.28): C, 70.80; H, 4.53; N, 17.38. Found: C, 71.31; H, 4.71; N, 17.22. MS (liquid mass), m/z : 1199.5 $[M - 5H_2O]^+$. UV-vis (pyridine): λ_{\max} ($\lg \epsilon$) = 360 nm (4.84), 394 sh, 640 (4.36), 687 (4.75). IR (cm^{-1}): 1725 w, 1650 w, 1600 vw, 1528 s, 1498 w, 1447 s, 1425 sh, 1388 w, 1318 s, 1300 (sh), 1275 s, 1180 s, 1165 s, 1120 vs, 1075 w, 1045 m, 1025 m, 1002 w, 990 m, 950 m, 925 sh, 845 w, 775 (sh), 760 vs, 712 vs, 692 vs, 415 vw. TGA revealed a weight loss of 6.6% in the temperature range of 25–150 °C (calcd for five molecules of water, 7.0%).

Tetrakis-2,3-(5,7-diphenyl-1,4-diazepino)porphyrazine Pentahydrate, $[Ph_8DzPzH_2] \cdot 5H_2O$, from Sodium or Lithium Salts. The salt $[Ph_8DzPzNa_2] \cdot 6H_2O$ (1.2 g, 0.90 mmol) was suspended in diluted hydrochloric acid (2.4 N) (10 mL), and the suspension was kept with stirring for 15 min. The precipitated dark green solid that formed was separated by filtration, washed with H_2O to neutrality and then with methanol, and brought to constant weight under vacuum. Yield: 0.98 g (85%). Calcd for $[Ph_8DzPzH_2] \cdot 5H_2O$, $C_{76}H_{60}N_{16}O_5$ (MW 1277.42): C, 71.46; H, 4.73; N, 17.54. Found: C, 71.11; H, 4.67; N, 17.10.

Alternatively, the free-base ligand could be obtained by using the lithium salt $[Ph_8DzPzLi_2] \cdot 5H_2O$ as a starting material under identical reaction conditions. Yield: 85%. Found: C, 71.20; H, 4.77; N, 17.17.

Tetrakis-2,3-(5,7-diphenyl-1,4-diazepino)porphyrinatocobalt(II) Tetrahydrate, $[Ph_8DzPzCo] \cdot 4H_2O$. A mixture of $[Ph_8DzPzNa_2] \cdot 6H_2O$ (82 mg, 0.06 mmol) and $Co(OCOCH_3)_2(H_2O)_4$ (86 mg, 0.35 mmol) was suspended in DMSO (2 mL) and kept at room temperature for 24 h with stirring. The solid was separated by centrifugation, washed with water until colorless washings and brought to constant weight under vacuum. Yield: 32 mg (40%). Calcd for $[Ph_8DzPzCo] \cdot 4H_2O$, $C_{76}H_{56}CoN_{16}O_4$ (MW 1316.32): C, 69.35; H, 4.29; N, 17.03. Found: C, 69.47; H, 4.56; N, 16.33. TGA revealed a weight loss of 5.9% (calcd for four molecules of H_2O , 5.5%).

Alternatively the Co^{II} complex could be obtained by using the lithium salt $[Ph_8DzPzLi_2] \cdot 5H_2O$ as a starting material by applying the same reaction conditions. Yield: 40%. Found: C, 70.31; H, 4.26; N, 16.95. TGA gave a water weight loss of 6.3% (calcd for four molecules of H_2O , 5.5%).

Cu^{II} and Zn^{II} complexes have been obtained from disodium or dilithium complexes similarly (see Supporting Information for details). Alternatively, by a similar procedure as earlier reported,⁷ the free-base ligand $[Ph_8DzPzH_2] \cdot 4H_2O$ was used for the synthesis of the Mn^{II} and Co^{II} complexes in pyridine or DMSO and of the Zn^{II} complex in DMSO (see details in Supporting Information).

Optical Limiting Measurements. In an experiment of OL measurements with the Z-scan technique, the intensity I of a Gaussian beam varies with the distance Z from the focus of the beam according to the relationship⁹

$$I(Z) = E/\tau w^2(Z)\pi \quad (1)$$

where E , τ , and $w(Z)$ are, respectively, the pulse energy (in joules), the pulse duration (in seconds) and the beam radius (in meters) as a function of the distance from the focus Z . The radius, w , of a Gaussian beam depends on the distance Z from the focus according to⁹

$$w^2(Z) = w_0^2 (1 + Z^2/Z_0^2) \quad (2)$$

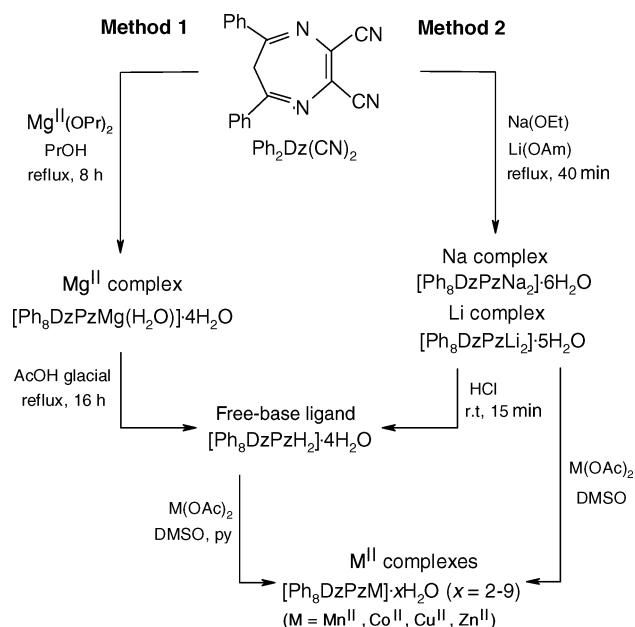
in which w_0 is the beam width at the focus and Z_0 is the diffraction length of the beam, defined as the ratio of the area $w_0^2\pi$ of the Gaussian beam at the focus to the laser beam wavelength λ . The OL performance of different species can be evaluated and meaningfully compared in terms of the variations of the normalized transmittance T/T_0 , defined as the ratio of intensity-dependent (T) to linear (T_0) transmittance. In a Z-scan experiment, such a property has its minimum value $(T/T_0)_{\min}$ at the focus ($Z = 0$), i.e., $(T/T_0)_{\min} = (T/T_0)_{Z=0}$. This corresponds to the beam location at which the level of irradiation is maximum. The use of the ratio $(T/T_0)_{\min}$ at a fixed wavelength as a critical parameter to evaluate the OL exhibited by different systems is meaningful provided that the linear transmittance T_0 is the same for all systems under examination. In general, the fulfillment of such a condition can require comparisons of the NLO properties of solutions with different concentrations of the active species, depending on the linear value of the molar extinction coefficient of the species in solution at the wavelength of interest.

The optical limiting (OL) effect for the various $[Ph_8DzPzM]$ species was studied in this work with the Z-scan technique in the open aperture configuration.⁸ Such a configuration allows for determination of the NLO effects associated solely with changes of the nonlinear absorption coefficient and not with changes of the nonlinear refractive index. For these measurements, solutions of the species in toluene were introduced in a quartz cuvette with an optical path thickness of 0.1 cm. The sample irradiation was carried out with a pulsed Nd:YAG laser (from Continuum Minilite, Edinburgh, Scotland) emitting at the second harmonic ($\lambda = 532$ nm). The maximum energy per laser pulse was 100 mJ. The pulse duration ranged over the interval 3–7 ns. The frequency of sample irradiation was 10 pulses/s. The Nd:YAG laser beam was focused with a neutral lens having a focal distance equal to 10 cm. During the Z-scan determinations, the sample spanned a total length of 3.5 cm centered at the beam focus. The displacement of the sample along the Z-scan direction was controlled by means of a piezoelectric driver. The laser beam radius was approximately 0.5 cm before lens focusing. The recording of sample transmittance was taken every 0.05 cm along the spanned length. The reported values of transmittance were averaged on the basis of 20 determinations per analyzed Z-position.

Electrochemical and Spectroelectrochemical Measurements. Cyclic voltammeter (CV) measurements were performed on an EG&G model 173 potentiostat coupled with an EG&E model 175 universal programmer in CH_2Cl_2 or pyridine solution containing 0.1 M TBAP as supporting electrolyte at 298 K. Pyridine and absolute CH_2Cl_2 were purchased from Aldrich Co. High-purity N_2 from Trigas was used to deoxygenate the solution before each electrochemical experiment. Tetrabutylammonium perchlorate (TBAP) was purchased from Sigma Chemical or Fluka Chemika Co., recrystallized from ethyl alcohol, and dried under vacuum at 40 °C for at least 1 week prior to use. A three-electrode system was used and consisted of a glassy carbon working electrode, a platinum wire counter electrode, and a saturated calomel reference electrode (SCE). The reference electrode was separated from the bulk solution by a fritted-glass bridge filled with the solvent, supporting electrolyte mixture. Thin-layer spectroelectrochemistry measurements were carried out at an optically transparent platinum thin-layer working electrode on a Hewlett-Packard model 8453 diode-array spectrophotometer coupled with an EG&G model 173 universal programmer. These measurements were carried out in solutions containing 0.2 M TBAP as supporting electrolyte.

Other Physical Measurements. IR spectra were taken with a Perkin-Elmer 783 spectrophotometer in the range 4000–200 cm^{-1} by using

Scheme 1



KBr pellets. UV–vis solution spectra were taken with a Varian Cary 5E spectrometer. Thermogravimetric analyses (TGA) were performed on a Stanton Redcroft model STA-781 analyzer in an N_2 atmosphere (0.5 L/min). FAB experiments were carried out on a multiple quadrupole instrument (VG quattro). MS (liquid mass) spectra were taken with a LC-MS Perkin-Elmer Sciex-API 365 at the Dipartimento di Chimica, Università “La Sapienza” (Rome). Low-temperature (80 K) EPR spectra were obtained on a Varian V 4502-4 spectrometer. Elemental analyses for C, H, and N were provided by Servizio di Microanalisi at the Dipartimento di Chimica, Università “La Sapienza” (Rome) on an EA 1110 CHNS-O instrument. X-ray powder diffraction patterns were obtained on a Philips PW 1710 diffractometer by use of $\text{Cu K}\alpha$ (Ni-filtered) radiation. Room-temperature magnetic susceptibility measurements were carried out by the Gouy method with a NiCl_2 solution as calibrant. The diamagnetic contribution of the free-base ligand $[\text{Ph}_8\text{DzPzH}_2] \cdot 4\text{H}_2\text{O}$ calculated from Pascal’s constants was -670×10^{-6} cgsu. The value obtained by taking 4 times that measured directly on the recrystallized monomer $\text{Ph}_2\text{Dz}(\text{CN})_2$ is -740×10^{-6} cgsu. This latter value was used for a correct calculation of the magnetic susceptibility of the complexes. Appropriate corrections for the diamagnetic contribution of specific metal ions and the water present were also made.

Results and Discussion

Synthetic and General Aspects, EPR, and Magnetic

Data: (a) Synthetic and General Aspects. In part 1 of this series⁷ we described the synthesis of the Mg^{II} complex $[\text{Ph}_8\text{DzPzMg}(\text{H}_2\text{O})] \cdot 4\text{H}_2\text{O}$ (for simplicity, hereafter all the diazepinoporphyrazine species will be formulated without clathrated water molecules), obtained by the template cyclotetramerization reaction of the precursor $\text{Ph}_2\text{Dz}(\text{CN})_2$ in the presence of Mg propylate, followed by its demetalation to give the free-base ligand $[\text{Ph}_8\text{DzPzH}_2]$. From this latter compound, the Cu^{II} and Zn^{II} complexes could be obtained by reaction with the corresponding metal acetates in pyridine solution⁷ (see Scheme 1, method 1). It is shown here that the Mn^{II} and Co^{II} complexes can be similarly obtained by using either pyridine or DMSO (Co) or pyridine (Mn) as a medium of the reaction (see Supporting Information Text S1 for details).

The synthetic pathway— Mg^{II} complex \rightarrow free-base ligand \rightarrow metal derivative—is a well-known procedure in the preparation

of tetrapyrrolic macrocycles such as phthalocyanines and other similar porphyrazine macrocyclic complexes, although being often time-consuming and frequently implying poor yields.³ The discovery that both the Na^{I} and Li^{I} derivatives of the present porphyrazine macrocycle can be prepared in high yield by direct cyclotetramerization of $\text{Ph}_2\text{Dz}(\text{CN})_2$ in the presence of sodium ethanolate and lithium amylate, respectively, opened a route to the use of these alkaline salts in metal exchange reactions with other metal salts (acetates). It is shown here that this procedure easily allows for room-temperature synthesis of the Mn^{II} , Co^{II} , Cu^{II} , and Zn^{II} complexes (Scheme 1, method 2), and an extension of the method also appears possible for several other metal derivatives.

As shown previously,⁷ and confirmed in this paper, all of the isolated complexes are hydrated amorphous materials, with the water molecules very likely being weakly ligated, presumably hydrogen-bonded, to the N atoms of the peripheral diazepine rings. Water can be eliminated by mild heating of the materials under vacuum. The amount of water ligated in a specific metal derivative is subject to some variability depending upon the particular sample under consideration. After the loss of water, thermogravimetric analyses show that the complexes are stable in an inert atmosphere up to temperatures of ca. 300 °C. Exposure of the samples to air leads to a rehydration of the materials. When either DMSO or pyridine was used as a medium of reaction, no evidence was seen for these S(O) or N donors to ligate at the central metal ion and form stable five- or six-coordinate adducts in the solid state. In all cases, attempts of sublimation under vacuum (10^{-2} – 10^{-3} mm Hg) at high temperature (400–500 °C) were unsuccessful; this was as expected, owing to the complex nature of the macrocycle, which is different from the essentially planar sublimable phthalocyanine $[\text{PcM}]$ species and the tetrakis(thiadiazole)porphyrazine complexes, $[\text{TTDPzM}]$.^{5a,b} The Na^{I} and Li^{I} species, $[\text{Ph}_8\text{DzPzNa}_2]$ and $[\text{Ph}_8\text{DzPzLi}_2]$, can be easily converted into the free-base ligand $[\text{Ph}_8\text{DzPzH}_2]$ by hydrolysis in air with diluted acid (HCl), water, or ethyl alcohol.

In preparation of the manganese species, the type of reaction product formed seems to depend on the nature of the solvent utilized. Reaction in pyridine under an inert atmosphere leads to the Mn^{II} complex, $[\text{Ph}_8\text{DzPzMn}]$, which appears, however, to undergo slow air oxidation to give a Mn^{III} species; the Mn^{II} species is also clearly converted to its oxidized form when dissolved in a noncoordinating solvent such as CHCl_3 (see discussion below). Use of DMSO as the reaction medium, for instance, leads to materials of uncertain composition, probably mixtures of Mn^{II} and Mn^{III} species, even if the reaction is carried out in an inert atmosphere.

(b) Room-Temperature Magnetic Susceptibility and EPR Data. Magnetic and EPR data for the Cu^{II} , Co^{II} , and Mn^{II} complexes are given in Table 1. The room-temperature magnetic moment of $[\text{Ph}_8\text{DzPzCu}]$ ($2.04 \mu_{\text{B}}$) is as expected for Cu^{II} (d^9), indicating the presence of one unpaired electron. The EPR spectrum of a solid sample prepared by diluting the Cu^{II} complex in the Zn^{II} analogue shows both hyperfine and superhyperfine structure (Figure 2A). The latter clearly establishes that there is an interaction of the unpaired electron with the nuclei of the four N atoms of the macrocycle surrounding the metal center.

The magnetic moment of the Co^{II} complex $[\text{Ph}_8\text{DzPzCo}]$ ($\sim 3.0 \mu_{\text{B}}$, Table 1) strongly suggests a d^7 low-spin state (one

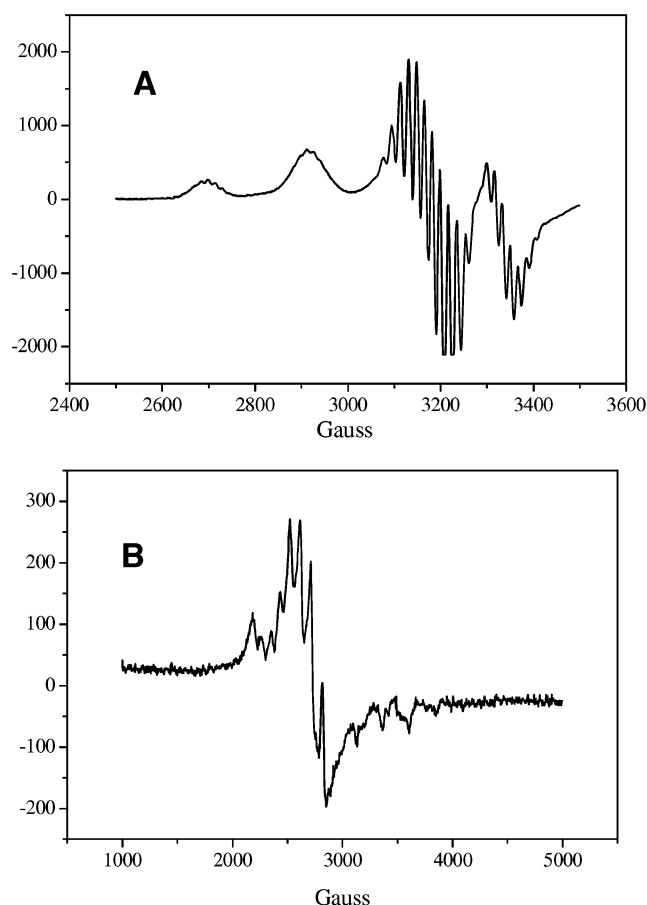


Figure 2. Low-temperature (80 K) EPR spectra of (A) $[\text{Ph}_8\text{DzPzCu}]$ and (B) $[\text{Ph}_8\text{DzPzCo}]$ obtained for samples magnetically diluted in the corresponding Zn^{II} matrix.

Table 1. Room-Temperature Magnetic Moments and Low-Temperature (80 K) EPR Data

complex ^a	μ_{eff}^b (μ_{B})	g_{\parallel}	g_{\perp}	A_{\parallel}^{M} (G)	A_{\perp}^{M} (G)	A_{\parallel}^{N} (G)
$[\text{Ph}_8\text{DzPzMn}](\text{H}_2\text{O})_5$ (py)	5.10					
$[\text{Ph}_8\text{DzPzCo}](\text{H}_2\text{O})_6$ (DMSO)	2.85					
$[\text{Ph}_8\text{DzPzCo}](\text{H}_2\text{O})_8$ (py)	3.05	2.181	2.611	238	91	
$[\text{Ph}_8\text{DzPzCu}](\text{H}_2\text{O})_5^c$ (DMSO)	2.04	2.149	2.046	220	18	~16

^a The solvent medium used for the synthesis is given in parentheses. ^b $\mu_{\text{eff}} = 2.84 \times (\chi_{\text{M}}'T)^{1/2}$. ^c Prepared from hydrated $[\text{Ph}_8\text{DzPzLi}_2]$.

unpaired electron) with the spin-only value ($1.73 \mu_{\text{B}}$) made significantly higher by additional paramagnetism. This is common to the findings for $[\text{PcCo}]$ ($2.69 \mu_{\text{B}}$)¹⁴ and, in general, for Co^{II} low-spin square-planar complexes ($\mu_{\text{eff}} = 2.2\text{--}2.9 \mu_{\text{B}}$).¹⁵ The EPR spectrum of a sample of $[\text{Ph}_8\text{DzPzCo}]$, also prepared by magnetic dilution, confirms the low-spin state for the metal center (Figure 2B). The g and A values are close to those found for $[\text{PcCo}]$ ¹⁶ and some detection of superhyperfine structure indicates that the unpaired electron is spending part of its time on the CoN_4 moiety with some delocalization on the N_4 system.

The μ_{eff} value of the Mn^{II} complex $[\text{Ph}_8\text{DzPzMn}]$ is intermediate between the spin-only magnetic moment expected for five ($5.92 \mu_{\text{B}}$) and three unpaired electrons ($\mu_{\text{eff}} = 3.87 \mu_{\text{B}}$), higher than for $[\text{PcMn}]$ ($4.34 \mu_{\text{B}}$, $S = 3/2$),¹⁴ and definitely lower

than what is found for Mn^{II} tetra[1,2,5-thia(seleno)diazolo]porphyrazines $[\text{TDPzMn}]$ ($5.98 \mu_{\text{B}}$)^{5b} and $[\text{TSeDPzMn}]$ ($5.88 \mu_{\text{B}}$),^{5d} these latter two values being indicative of a high-spin configuration. Additional studies on the temperature dependence of the magnetic moment for the present Mn^{II} species may be needed to explain whether the observed intermediate magnetic moment depends exclusively on the electronic situation of the metal center in the molecule or on some type of interunit metal–metal magnetic exchange.

UV–Visible Spectra. The UV–visible spectra of the free-base ligand, $[\text{Ph}_8\text{DzPzH}_2]$, and its complexes with Mg^{II} , Cu^{II} , and Zn^{II} were reported quantitatively in basic media (pyridine) and qualitatively in neutral (CHCl_3), slightly acidic (CH_3COOH), or acidic solutions (CF_3COOH and 96% H_2SO_4).⁷ Similarly, quantitative (pyridine) and qualitative spectral data in CHCl_3 and in the same acidic solutions (CH_3COOH , CF_3COOH , and H_2SO_4) were taken for the new Mn^{II} , Co^{II} , Li^{I} , and Na^{I} complexes (see Supporting Information, Text S1 and Tables S1 and S2).

The general aspect of the UV–visible spectra of the diazepinoporphyrazines $[\text{Ph}_8\text{DzPzM}]$ partly recalls that normally observed for the related phthalocyanine macrocycles¹⁷ or their aza analogues;³ among these latter compounds are the recently described tetrakis[1,2,5-thia(seleno)diazole]porphyrazines,⁵ which show intense Soret and Q bands, assigned as $\pi \rightarrow \pi^*$ transitions, and located in the spectral regions 350–400 and 630–650 nm, respectively. The interesting new characteristic spectral feature for the presently reported species is the presence of an additional absorption band in the Q -band region, at 660–680 nm. This band clearly appears in the spectra measured in basic, neutral, or slightly acidic solvents (e.g., in pyridine, CHCl_3 , and CH_3COOH ; see representative spectra in Figure 3 for $[\text{Ph}_8\text{DzPzCo}]$). This absorption, also detected and discussed in detail for the previously reported diazepinoporphyrazines,⁷ is assigned as an $n \rightarrow \pi^*$ transition (Q_n band), discarding alternative assignments (see further discussion below).

The occurrence of low-energy-lying $n \rightarrow \pi^*$ transition bands of moderate-to-high intensity is not unusual for porphyrazines carrying heteroatoms directly attached to the β -pyrrole positions, and both the position and intensity of the $n \rightarrow \pi^*$ transition are strongly dependent upon the type of heteroatom and the steric orientation of the associated lone pair(s). If the base N-atom lone pairs are located in the plane of the macrocycle, i.e., perpendicular to the π molecular orbitals, as is the case, for instance, for pyridino- or pyrazinoporphyrazines, the $n(\text{N}) \rightarrow \pi^*$ transitions are z -polarized and appear only as weak bands. According to both theoretical and experimental results, these transitions are responsible for the broadening and diffuse character of the Soret band¹⁸ and can also contribute to the low-intensity absorption on the blue side of the Q band.¹⁹ In contrast, the situation can become markedly different when the lone

- (17) Stillman, M. J. In *Phthalocyanines: Properties and Applications*; Leznoff, C. C., Lever, A. B. P., Eds.; VCH Publishers: New York, 1989; Vol. 1, pp 133–289.
- (18) (a) Henriksson, A.; Roos, B.; Sundbom, M. *Theor. Chim. Acta* **1972**, *27*, 303. (b) Henriksson, A.; Sundbom, M. *Theor. Chim. Acta* **1972**, *27*, 213. (c) Schaffer, A. M.; Gouterman, M.; Weiss, C. *Theor. Chim. Acta* **1973**, *30*, 9. (d) Dvornikov, S. S.; Knyukshto, V. N.; Kuzmitski, V. A.; Shulga, A. M.; Solovyov, K. N. *J. Luminesc.* **1981**, *23*, 373.
- (19) (a) Huang, T. H.; Reickhoff, K. E.; Voigt, E. M. *J. Chem. Phys.* **1982**, *77*, 3424. (b) Huang, T. H.; Reickhoff, K. E.; Voigt, E. M. *J. Phys. Chem.* **1981**, *85*, 3322. (c) Mack, J.; Stillman, M. J. *J. Phys. Chem.* **1995**, *99*, 7935. (d) Mack, J.; Stillman, M. J. *Coord. Chem. Rev.* **2001**, *219–221*, 993–1032.

(14) Lever, A. B. P. *J. Chem. Soc.* **1965**, 1821.

(15) Figgis, B. M.; Nyholm, R. S. *J. Chem. Soc.* **1954**, 12.

(16) Assour, J. M. *J. Am. Chem. Soc.* **1965**, *87*, 4701, and references therein.

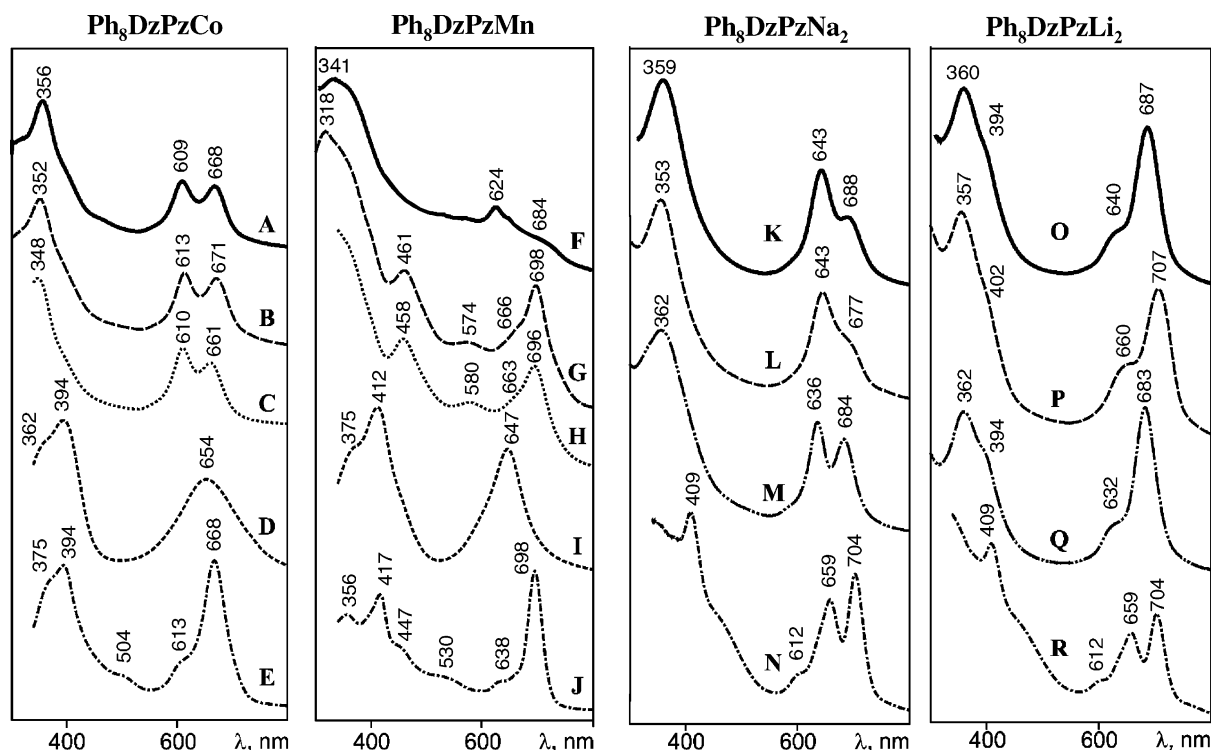


Figure 3. UV-vis spectra of [Ph₈DzPzCo] (A–E), [Ph₈DzPzMn] (F–J), [Ph₈DzPzNa₂] (K–N), and [Ph₈DzPzLi₂] (O–R) in pyridine (A, F, K, and O), CHCl₃ (B, G, L, and P), DMSO (M and Q), CH₃COOH (C and H), CF₃COOH (D and I), and H₂SO₄ (E, J, N, and R).

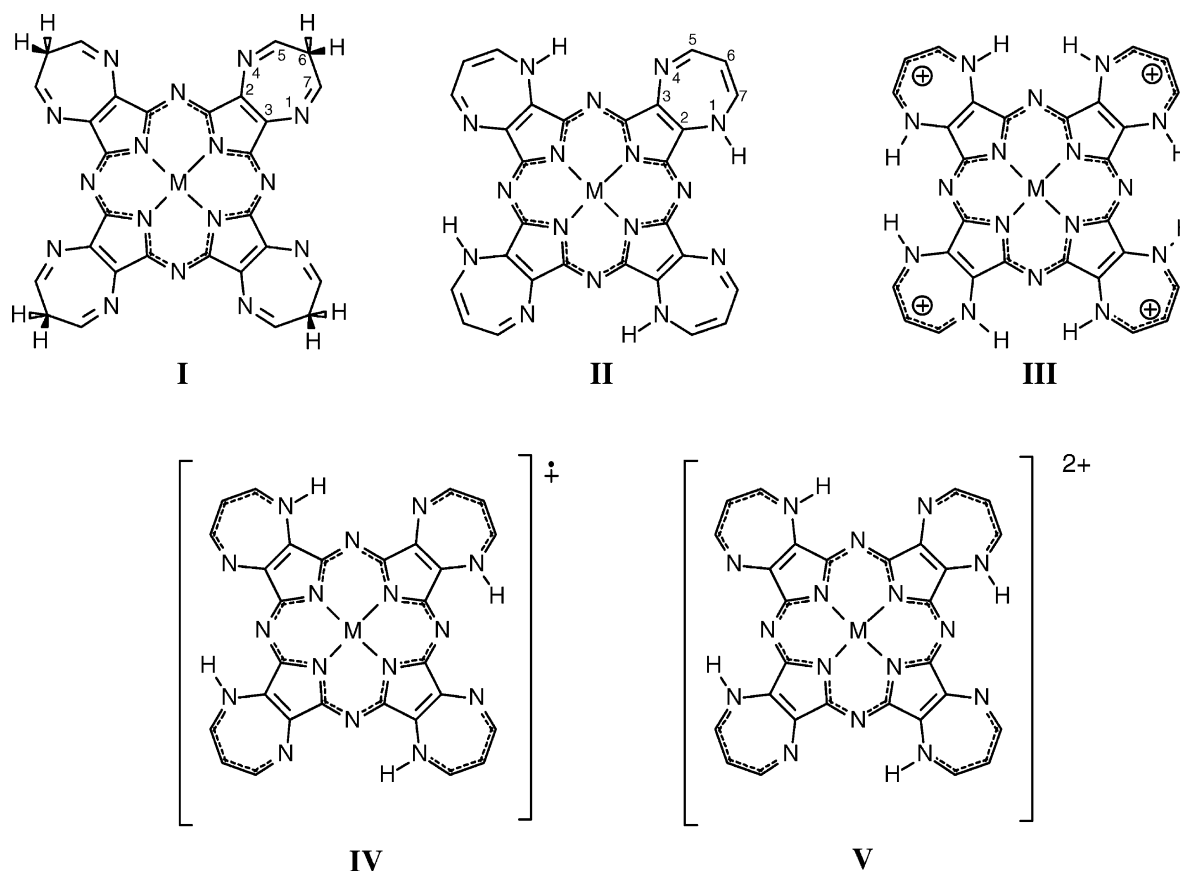
pair(s) of the heteroatom(s), owing to their out-of-plane orientation, can be directly involved in conjugation with the macrocyclic π -system. For a number of recently reported porphyrazine macrocycles carrying O, S, or N atoms directly attached to the β -carbon atoms in, respectively, alkoxy-,^{20,21} alkylthio-,^{20,22} and dialkylamino-substituted^{23,24} porphyrazines (including also diazepinoporphyrazines²⁵ strictly recalling the present species), the noncoplanar arrangement of the lone pairs of the mentioned heteroatoms is associated with a gain in intensity of the associated $n \rightarrow \pi^*$ transitions. Also, the transitions can be found at wavelengths well above the classical Soret range (300–400 nm) and, especially in the case of dialkylaminoporphyrazines, extending into the Q -band region. The intensity of the $n \rightarrow \pi^*$ transitions for these latter species becomes comparable or even higher than that of the lowest $\pi \rightarrow \pi^*$ transition. Moreover, since the eight dialkylamino groups are not present in a fixed equivalent conformation, both the $n \rightarrow \pi^*$ and the $\pi \rightarrow \pi^*$ transition bands are broadened and have a diffuse character.^{23–25} Going back to the presently investigated diazepinoporphyrazines, the N atom's lone pairs of the boat-shaped diazepine rings in the 6*H* form (see Figure 1) are forced to an out-of-plane orientation with respect to the macrocyclic ring. Thus, they can be involved in partial conjugation with the central π -chromophore.

As a consequence, the $n \rightarrow \pi^*$ transitions can mix with the $\pi \rightarrow \pi^*$ transitions and gain in intensity, appearing in the Q -band region as a nondiffuse Q_n band of moderate intensity.

Indeed, as an alternative hypothesis, a splitting of the Q band might be suggested as the reason for the presence of two absorptions in the Q -band area. It should be considered, however, that a splitting of the Q band for porphyrazines is usually caused by effects due to the excitonic π – π coupling in dimacrocyclic systems, e.g., (Pc)₂M, (PcM)₂, or (PcM)₂(X),²⁶ or it may originate from the symmetry reduction of the π -chromophore from D_{4h} to D_{2h} or lower when the molecule loses its 4-fold axis of symmetry and the two lowest unoccupied molecular orbitals (LUMO) are no longer degenerate. In the metal complexes, this can be due to unsymmetrical substitution and/or annulation in the β -pyrrole positions.^{27,28} On the other hand, an out-of-plane position of the metal atom (C_{4v} symmetry) or a severe distortion from planarity of the π -chromophore, which can occur due to the steric interaction of the bulky substituents in the annulated rings (e.g., in octaalkyl-²⁹ and octapentyl-^{28,30} substituted phthalocyanines), results only in a bathochromic shift of the Q -band maximum [since the highest occupied molecular orbital (HOMO) is destabilized] and not in

- (20) Forsyth, T. P.; Williams, D. B. G.; Montalban, A. G.; Stern, C. L.; Barrett, A. G. M.; Hoffman, B. M. *J. Org. Chem.* **1998**, *63*, 331.
 (21) Bellec, N.; Montalban, A. G.; Williams, D. B. G.; Cook, A. S.; Anderson, M. E.; Feng, X.; Barrett, A. G. M.; Hoffman, B. M. *J. Org. Chem.* **2000**, *65*, 1774.
 (22) Ehrlich, L. A.; Skrdla, P. J.; Jarrell, W. K.; Sibert, J. W.; Armstrong, N. R.; Saavedra, S. S.; Barrett, A. G. M.; Hoffman, B. M. *Inorg. Chem.* **2000**, *39*, 3963.
 (23) Goldberg, D. P.; Montalban, A. G.; White, A. J. P.; Williams, D. J.; Barrett, A. G. M.; Hoffman, B. M. *Inorg. Chem.* **1998**, *37*, 2873.
 (24) Beall, L. S.; Mani, N. S.; White, A. J. P.; Williams, D. J.; Barrett, A. G. M.; Hoffman, B. M. *J. Org. Chem.* **1998**, *63*, 5806.
 (25) Baum, S. M.; Trabanco, A. A.; Montalban, A. G.; Micallef, A. S.; Zhong, C.; Meunier, H. G.; Suhling, K.; Phillips, D.; White, A. J. P.; Williams, D. J.; Barrett, A. G. M.; Hoffman, B. M. *J. Org. Chem.* **2003**, *68*, 1665.

- (26) See for example (a) (Pc)₂Bi: Ostendorp, G.; Homborg, H. *Z. Anorg. Allg. Chem.* **1996**, *622*, 873. (b) (PcRh)₂: Hueckstaedt, H.; Bruhn, C.; Homborg, H. *J. Porphyrins Phthalocyanines* **1997**, *1*, 367. (c) (PcFe)₂(μ -C) and (PcRu)₂(μ -C): Kienast, A.; Galich, L.; Murray, K. S.; Moubarak, B.; Lazarev, G.; Cashion, J. D.; Homborg, H. *J. Porphyrins Phthalocyanines* **1997**, *1*, 141.
 (27) Kobayashi, N.; Konami, H. In *Phthalocyanines: Properties and Applications*; Leznoff, C. C.; Lever, A. B. P., Eds.; VCH Publishers: New York, 1996; Vol. 4, pp 343–404.
 (28) Donzello, M. P.; Ercolani, C.; Gaberkorn, A. A.; Kudrik, E. V.; Meneghetti, M.; Marcolongo, G.; Rizzoli, C.; Stuzhin, P. A. *Chem. Eur. J.* **2003**, *9*, 4009.
 (29) Chambrier, I.; Cook, M. J.; Wood, P. T. *J. Chem. Soc., Chem. Commun.* **2000**, 2133.
 (30) Stuzhin, P. A.; Kudrik, E.; Comelissen, U.; Homborg, H. 2nd International Conference on Porphyrins and Phthalocyanines, ICPP-2, Kyoto, Japan, June 30–July 5, 2002; P-291, p 539.

Chart 1. Tautomeric (**I** and **II**), Protonated (**III**), and Oxidized Forms (**IV** and **V**) of the Species $[\text{Ph}_8\text{DzPzM}]^a$ 

^a Numbering of atoms in the diazepine rings is exemplified for forms **I** (abbreviated $[\text{Ph}_8(6\text{HDz})\text{PzM}]$) and **II** (abbreviated $[\text{Ph}_8(1\text{HDz})\text{PzM}]$). Phenyl groups present in positions 5 and 7 of each diazepine ring are omitted for clarity.

a splitting of the Q band. Since, as was evidenced from ^1H NMR measurements,⁷ the metal complexes of the investigated diazepinoporphyrazine species have (at least formally) an effective D_{4h} symmetry of the central π -chromophore and no dimerization effects have been detected (even in more concentrated solutions than those usually used for UV-vis measurements), the alternative hypothesis considered, i.e., splitting of the Q -band, does not appear to apply to the present macrocycles.

The influence of the solvent on the UV-vis spectral features of diazepinoporphyrazines was previously discussed in relationship with the possible occurrence of tautomeric (Chart 1, **I** and **II**) or protonated forms (Chart 1, **III**) of the diazepine rings.⁷ In slightly basic (pyridine), neutral (CHCl_3 , DMSO), or even slightly acidic solvents (CH_3COOH), the interaction of the diazepine rings with the solvent is weak. Thus, the macrocycles display, peripherally, the more stable 6H tautomeric form **I** (Chart 1) and the skeletal formulation can be given as $[\text{Ph}_8(6\text{HDz})\text{PzM}]$. In connection with form **I**, for the Co^{II} complex for instance, both Q and Q_n bands are observed in the UV-vis spectrum (Figure 3A–C). As is usual for $n \rightarrow \pi^*$ transitions, a fact also observed here (see Figure 3), the peak position of the Q_n bands exhibits a stronger solvatochromic effect than in the case of the Q bands ($\pi \rightarrow \pi^*$ transition).

The situation in strong acids is different, as discussed earlier.⁷ In CF_3COOH , specific acid solvation determines the stability of the diazepine ring in the 1H tautomeric form and a broad Q band appears as seen in Figure 3D, again for the Co^{II} species, written as $[\text{Ph}_8(1\text{HDz})\text{PzCo}]$ and represented by form **II** in Chart

1. The diazepine ring in the 1H form, unlike the 6H form, is more planar and has two types of lone pairs, one belonging to imido ($-\text{N}=\text{C}$) and one to amino ($-\text{NH}-$) nitrogens. This gives rise to the corresponding $n(\text{N}) \rightarrow \pi^*$ transitions leading to the broadening and diffuse character of the Q band. Protonation of the 1H diazepine rings occurs in H_2SO_4 , resulting in the formation of the highly symmetric tetracationic species $[\text{Ph}_8(1\text{HDzH})\text{PzCo}]^{4+}$ (**III**, Chart 1). In this formulation of the diazepine ring, one N atom is protonated and another provides its lone pair for the formation of the external quasi-aromatic 6π -electron diazepinium cation.³¹ Thus, no $n(\text{N}) \rightarrow \pi^*$ transition from the diazepine N-atoms to the porphyrazine macrocycle can take place and the observed spectrum is similar to that of the phthalocyanine systems in that it shows intense $\pi \rightarrow \pi^*$ absorptions (Soret and Q bands) and the absence of $n \rightarrow \pi^*$ bands in the low-energy UV-visible region (Figure 3E).

The UV-vis spectral features of the Mn^{II} , Li^{I} and Na^{I} complexes need some specific comments. The Mn^{II} complex, $[\text{Ph}_8\text{DzPzMn}]$, shows a broad absorption envelope in pyridine which is spread over the whole UV-vis region (Figure 3F), with the Q band appearing as a weak peak at 624 nm; a similar broad band is attributable to the Q_n transition in the region 680–700 nm and additional charge-transfer bands appear at higher wavelengths (> 800 nm), as is also the case for $[\text{PcMn}]^{17}$ and the Mn^{II} porphyrazine $[\text{Ph}_8\text{PzMn}]$.³² Dissolution of $[\text{Ph}_8$

(31) Loyd, D.; Marshall, D. R. *Chem. Ind.* **1964**, 1760.

(32) Stuzhin, P. A.; Hamdush, M.; Homborg, H. *Mendeleev Commun.* **1997**, 5, 196.

DzPzMn] in CHCl_3 results fairly quickly in formation of a Mn^{III} species (probably $[\text{Ph}_8\text{DzPzMnCl}]$), as indicated by the observed spectral changes (Figure 3G), i.e., a new Q -band maximum at 698 nm, shoulders at ca. 574 and 461 nm and a progressive concomitant disappearance of all bands of the initial spectrum. Moreover, the final spectrum closely resembles the spectra of Mn^{III} porphyrazines³² and phthalocyanines.^{17,33} Noticeably, a reverse change of the spectrum from that of the oxidized species to that of $[\text{Ph}_8\text{DzPzMn}]$ is observed by addition of pyridine to the CHCl_3 solution. The above observations point to a facile electron exchange process involving the $\text{Mn}^{\text{II}}/\text{Mn}^{\text{III}}$ redox couple, Mn^{II} being more stable in pyridine but easily oxidized to Mn^{III} in the noncoordinating CHCl_3 .

The presence of both Q and Q_n bands for the Mn^{II} complex in pyridine (624 and 684 nm) is consistent with the formula $[\text{Ph}_8(6\text{HDz})\text{PzMn}]$, i.e., with the presence of the diazepine rings in the 6H tautomeric form, as is found also for the Co^{II} and the other M^{II} derivatives⁷ (see Table S1 and Text S1 in Supporting Information). It should be pointed out that the position of the Q -band maximum for the Mn^{II} species in pyridine (624 nm) approaches what is found for the other M^{II} analogues (610–640 nm), whereas in the case of the suggested Mn^{III} complex, in CHCl_3 $[\text{Ph}_8\text{DzPzMnCl}]$, the Q band (Figure 3G) is bathochromically shifted (698 nm), a fact common to other Mn^{III} porphyrazine analogues.^{32–34} The presence of charge-transfer bands (461 and 574 nm) in the spectrum of the suggested $[\text{Ph}_8\text{DzPzMnCl}]$ in CHCl_3 and the absence of absorptions on the red side of the Q band are also features characteristic of pentacoordinated Mn^{III} porphyrazines.³⁴ The lack of a Q_n band in the spectrum of the Mn^{III} species suggests that the peripheral diazepine rings are in the 1H tautomeric form and the complex can then be more precisely formulated as $[\text{Ph}_8(1\text{HDz})\text{PzMnCl}]$. The occurrence of 6H–1H tautomerism of the diazepine rings associated with the $\text{Mn}^{\text{II}}/\text{Mn}^{\text{III}}$ oxidation can be related to changes in the $d\pi$ – $p\pi$ interaction between the metal and the macrocyclic ligand since the 1H form provides more extensive conjugation.

The spectra of $[\text{Ph}_8\text{DzPzMn}]$ in acidic media are quite similar to (CH_3COOH , Figure 3H), or resemble (CF_3COOH , H_2SO_4 , Figure 3, spectra I and J, respectively) the final spectrum of the species in CHCl_3 (Figure 3G). This indicates that oxidation of the metal center easily occurs under acidic conditions. The spectra in CF_3COOH and H_2SO_4 also closely resemble the spectra of the other Co^{II} , Cu^{II} , and Zn^{II} analogues, in keeping with the occurrence of the tautomeric 1H form in acidic media,⁷ and deserve no further discussion. Nevertheless, it is here reiterated that the bathochromic shift of the Q -band position in H_2SO_4 (698 nm) in comparison with findings for the other M^{II} complexes (660–670 nm), as well as the presence of the CT bands at ca. 447 and 530 nm, is closely related to the presence of Mn^{III} and suggests the formation of the tetracation $[\text{Ph}_8(1\text{HDzH})\text{PzMn}^{\text{III}}(\text{X})]^{4+}$ ($\text{X} = \text{HSO}_4^-$) in this strongly acidic medium.

The spectra of the Na^{I} and Li^{I} species are different from one another, in both basic (pyridine) and neutral (CHCl_3 , DMSO) solutions. The spectra of the Na^{I} derivative in these solvents (Figure 3K–N) clearly show the presence of Q and Q_n bands,

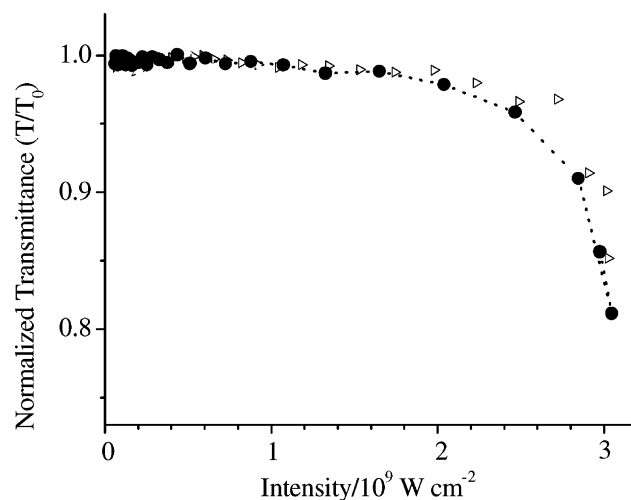


Figure 4. Optical limiting curve for the species $[\text{Ph}_8\text{DzPzCu}]$ ($T_0 = 90\%$ at the concentration 4.5×10^{-5} M).

a fact that suggests for the macrocycle the 6H tautomeric form **I**, i.e., $[\text{Ph}_8(6\text{HDz})\text{PzNa}_2]$. The Li^{I} derivative possesses the classic spectrum, i.e., with only Soret and Q bands (Figure 3O–R). The long-wavelength position of the Q band seems to indicate the occurrence of the 1H tautomeric form **II**; thus, the complex is formulated as $[\text{Ph}_8(1\text{HDz})\text{PzLi}_2]$. Not surprisingly, the position of the Q band for this alkaline derivative moves bathochromically as a function of the solvent (683 nm in DMSO, 687 nm in pyridine, and 707 nm in CHCl_3). This is probably related to the effect of solvation on the N–H bonds in the 1H tautomeric form. Of course, this basic solvation is less relevant for the 6H tautomeric form present in all of the other $[\text{Ph}_8(6\text{HDz})\text{PzM}]$ complexes, for which, in fact, the Q band seems to undergo a more limited solvatochromic effect. Finally, the spectra of the Na^{I} and Li^{I} complexes in acidic media (CH_3COOH , CF_3COOH , 96% H_2SO_4) are clearly indicative of their full conversion into the free-base ligand $[\text{Ph}_8\text{DzPzH}_2]$ (see Table S2 and Figure 3N and R), as would be expected.

OL Measurements. It is shown here that the investigated diazepinoporphyrazines exhibit NLO properties at the wavelength 532 nm owing to the observed transmittance changes of their solutions, which occur at different levels of irradiation as determined in Z-scan experiments.³⁵ Solutions of compounds in the series $[\text{Ph}_8\text{DzPzM}]$ behave like reverse-saturable absorbers (RSAs),^{9,36} i.e., like systems that become more opaque and absorbing as the intensity of irradiation increases.³⁷ Such an effect results in a reversible decrease of the system transmittance with increasing incident light intensity (see Figure 4 for the case of the Cu^{II} complex).⁹

Analogous compounds showing such a phenomenon are generally described as molecular dynamic filters with photo-generated excited states strongly light-absorbing.^{38,39} As an extension, we can then reasonably assume that the mechanism of the excited-state absorption⁹ remains valid when the OL effect generated by the $[\text{Ph}_8\text{DzPzM}]$ species has to be analyzed. The

(35) Sauter, E. G. *Nonlinear Optics*, Wiley: New York, 1996.

(36) Giuliano, C. R.; Hess, L. D. *IEEE J. Quantum Electron.* **1967**, *3*, 358.

(37) Blau, W.; Byrne, H.; Dennis, W. M.; Kelly, J. M. *Opt. Commun.* **1985**, *56*, 25.

(38) Van Stryland, E. W.; Sheik-Bahae, M.; Said, A. A.; Hagan, D. J. *Prog. Cryst. Growth Charact.* **1993**, *27*, 279.

(39) Shirik, J. S.; Pong, R. G. S.; Bartoli, F. J.; Snow, A. W. *Appl. Phys. Lett.* **1993**, *63*, 1880.

(33) Dolotova, O. V.; Bundina, N. I.; Kaliya, O. L.; Lukyanets, E. A. *J. Porphyrins Phthalocyanines* **1997**, *1*, 355.

(34) Klueva, M. E.; Stuzhin, P. A.; Berezin, B. D. *Russ. J. Coord. Chem.* **2003**, *29*, 189–195.

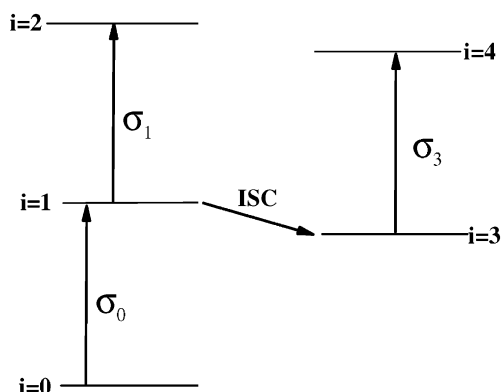


Figure 5. Electronic energy level diagram for a five-level system.^{9,38} The electronic states associated with energy levels $i = 0, 1, 2$ are singlet states. The electronic states associated with energy levels $i = 3, 4$ are triplet states. The symbol σ_i represents the absorption cross section for the electronic transition between the i th level (lower energy) and the $(i + 1)$ th level (upper energy). ISC represents the process of intersystem crossing from singlet to triplet states. For the sake of clarity, the various relaxation processes of fluorescence, $[2 \rightarrow 1]$, $[1 \rightarrow 0]$, $[4 \rightarrow 3]$, and phosphorescence, $[3 \rightarrow 0]$, are omitted.

fundamental processes at the basis of the reverse-saturable absorption are essentially two consecutive transitions ($[0 \rightarrow 1]$ and $[1 \rightarrow 2]$ or alternatively $[0 \rightarrow 1]$ and $[3 \rightarrow 4]$, depending on the lifetimes of the states and the light pulse duration), as depicted in the generalized five-level model of nonlinear absorption (Figure 5).^{9,38}

For practical purposes,³⁸ a parameter of interest for the evaluation of the OL performance by different optical systems is the minimum value of transmission achievable by the system in defined conditions of irradiation. For solutions of the various $[\text{Ph}_8\text{DzPzM}]$ macrocycles, the minimum values of transmission range over a quite wide interval corresponding to about 50–85% of the linear transmission value depending upon the nature of the central metal, M. Hence, such a considerable variation shows that the nature of the coordinating central metal M plays a prominent role in determination of the NLO transmission, similar to the behavior observed for other conjugated tetrapyrrolic macrocycles.⁴⁰

Figure 6 reports the Z-scan profiles of $[\text{Ph}_8\text{DzPzM}]$ with $M = \text{Mn}^{\text{II}}, \text{Co}^{\text{II}}, \text{Cu}^{\text{II}}, \text{Zn}^{\text{II}}$, and $\text{Mg}^{\text{II}}(\text{H}_2\text{O})$. The value of T_0 was 92% for all solutions. From this plot it is found that the parameter $(T/T_0)_{\text{min}} = (T/T_0)_{Z=0}$ increases for the different $[\text{Ph}_8\text{DzPzM}]$ complexes with M in the following order: $\text{Zn}^{\text{II}} < \text{Mn}^{\text{II}} < \text{Cu}^{\text{II}} < \text{Co}^{\text{II}}$ (Figure 6A). Since the lower the value of $(T/T_0)_{\text{min}}$, the better the OL effect, this would correspond to a decrease of such an effect in passing from $[\text{Ph}_8\text{DzPzZn}]$ to $[\text{Ph}_8\text{DzPzCo}]$. If the five-level model is taken into account (Figure 5), such differences in the OL effect generated by the series of species in Figure 6A could be mostly ascribed to differences of the kinetics of the intersystem crossing (ISC) process that occurs when the succession of the electronic transitions is $[0 \rightarrow 1]$ and $[3 \rightarrow 4]$ (Figure 5).⁴¹ The ISC process can be accelerated if the central atom of the complex possesses a high number of polarizable electrons (heavy atom effect) and/or gives

rise to strong effects of spin–orbit coupling.⁴¹ The better OL effect achieved with $[\text{Ph}_8\text{DzPzZn}]$ as compared to the other compounds is ascribed to the relatively high polarizability of the Zn^{II} electronic cloud inferred by the higher number of d electrons and the completeness of d orbital filling. Such features allow an effective screening of the positive charge of the coordinating Zn and favor the transition that is at the basis of the OL effect at 532 nm produced by these kinds of complexes in the excited state.⁴² On the other hand, the stronger OL effect exhibited by $[\text{Ph}_8\text{DzPzMn}]$ with respect to $[\text{Ph}_8\text{DzPzCu}]$ and $[\text{Ph}_8\text{DzPzCo}]$, both of which have metal centers with a higher number of d electrons, is basically due to its very high magnetic moment ($> 4 \mu_B$) for the higher number of unpaired electrons. This feature accelerates the ISC process, i.e., the $[1 \rightarrow 3]$ transition (Figure 5), and allows faster formation of the highly absorbing triplet state with energy level 3.^{41,43} The OL effect exhibited by $[\text{Ph}_8\text{DzPzCu}]$ is better than for $[\text{Ph}_8\text{DzPzCo}]$, due mostly to the higher number of d electrons (d^9 vs d^7), which infers higher electronic polarizability to the central atom. These results seem to fit well with predictions. In fact, in a study of the OL effect generated by metal-conjugated macrocyclic complexes,⁴⁴ it was usually verified that the higher the electronic polarizability of the metal center, the shorter the lifetime of the first excited state (level 1, Figure 5) and the higher the yield of formation of the absorbing triplet excited state (level $i=3$, Figure 5). Thus, in the absence of spin–orbit coupling effects associated with the paramagnetism of the central atom,⁴² the OL effect at 532 nm is normally found to be more pronounced for complexes of transition metals in which the coordinating central metal is more electron-rich.^{42,44} It is known that the lifetimes of the first triplet state ($i = 3$ in Figure 5) of complexes such as porphyrins, porphyrazines, and analogues are dependent on the nature of the coordinating central metal M with Zn^{II} complexes displaying the higher values of triplet-state lifetimes.⁴⁵ On the other hand, the values of the triplet-state lifetimes in these complexes are usually not lower than 1 μs ,⁴⁶ i.e., 100 times larger than the laser pulse duration used in the present investigation. Under these conditions it is expected that the variation of the triplet-state lifetimes within the series of compounds $[\text{Ph}_8\text{DzPzM}]$ with $M = 2\text{H}, \text{Mg}^{\text{II}}(\text{H}_2\text{O}), \text{Mn}^{\text{II}}, \text{Co}^{\text{II}}, \text{Cu}^{\text{II}}$, and Zn^{II} , does not account for the observed variations of the OL effectiveness.

The Z-scan profiles of $[\text{Ph}_8\text{DzPzMg}(\text{H}_2\text{O})]$ and $[\text{Ph}_8\text{DzPzZn}]$ are counterpart in Figure 6B in order to compare the effects of different kinds of closed electron shells (s^2p^6 and d^{10}) on the resulting OL effect produced by these complexes. The observed behavior, i.e., $(T/T_0)_{\text{min}}\{\text{Zn}\} < (T/T_0)_{\text{min}}\{\text{Mg}\}$, can be mostly ascribed to the higher number and polarizability of electrons present in a closed d shell (Zn^{II}) than in closed s and p shells (Mg^{II}). In such a comparison, a more effective screening of the positive charge of the coordinating Zn^{II} with respect to Mg^{II} is determined, thus favoring for the former compound the occurrence of the electronic transition responsible for the OL effect

(40) Shirik, J. S. S.; Lindle, J. R.; Bartoli, F. J.; Kafafi, Z. H.; Snow, A. W. In *Materials for Nonlinear Optics—Chemical Perspectives*; Marder, S. R., Sohn, J. E., Stucky, G. D., Eds.; ACS Symposium Series 455; American Chemical Society: Washington, DC, 1991; p 626.
 (41) Perry, J. W.; Mansour, K.; Lee, I. Y. S.; Wu, X. L.; Bedworth, P. V.; Chen, C. T.; Ng, D.; Marder, S. R.; Miles, P.; Wada, T.; Tian, M.; Sasabe, H. *Science* **1996**, *479*, 89.

(42) Cheng, W. D.; Wu, D.-S.; Zhang, H.; Chen, J. T. *Phys. Rev. B* **2001**, *64*, 125109/1.
 (43) Turro, N. J. *Molecular Photochemistry*; Benjamin: Reading, MA, 1977.
 (44) Perry, J. W.; Mansour, K.; Marder, S. R.; Perry, K. J.; Alvarez, D.; Choong, I. *Opt. Lett.* **1994**, *19*, 625.
 (45) (a) Harryman, A. J. *Chem. Soc., Faraday Trans. 2* **1981**, *77*, 1281. (b) Rihter, B. D.; Bohorquez, M. D.; Rodgers, M. A. J.; Kenney, M. E. *Photochem. Photobiol.* **1992**, *55*, 677. (c) Kalyanasundaram, K.; Neumann-Spallart, M. *J. Phys. Chem.* **1982**, *86*, 5163.
 (46) Kosonocky, W. F.; Harrison, S. E.; Stander, R. J. *Chem. Phys.* **1965**, *43*, 831.

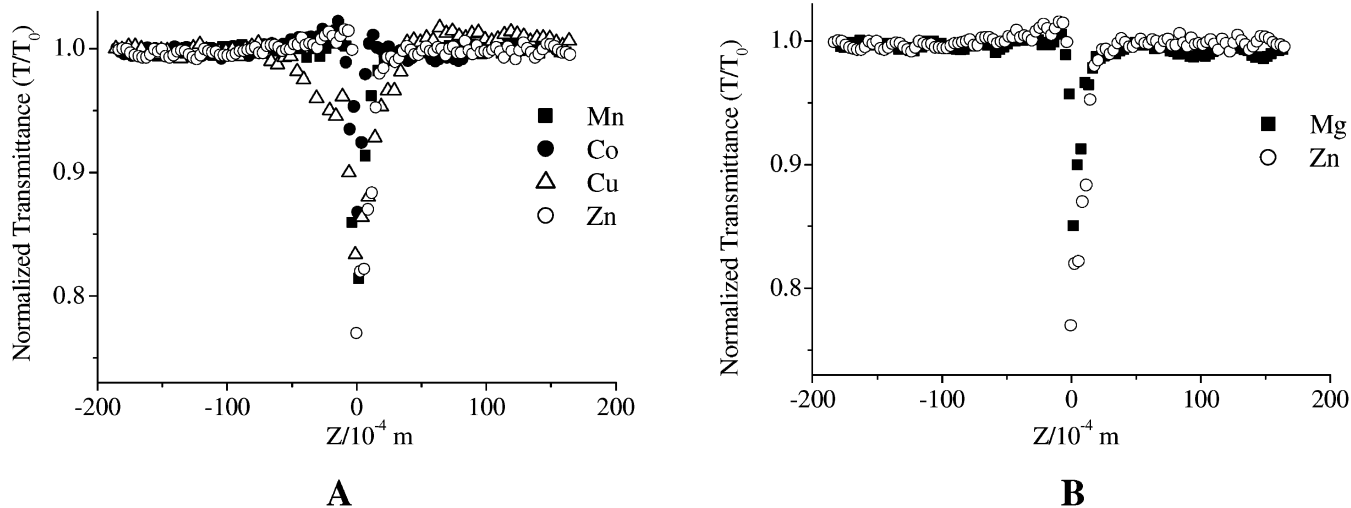


Figure 6. Z-scan profiles of [Ph₈DzPzM]: (A) M = Mn^{II}, Co^{II}, Cu^{II}, and Zn^{II}; (B) M = Mg^{II}(H₂O) and Zn^{II}. The value of T₀ is 92% for all the species. Solution concentrations were in the range (3.5–4.5) × 10⁻⁵ M.

at 532 nm, observed for axially unsubstituted conjugated macrocyclic metal complexes in the excited state.⁴² Such an excited-state transition has been described as a combination of π–π* (intraligand transition) and ligand-to-metal charge transfer (LMCT).⁴²

The OL effect could also be verified by irradiation of [Ph₈-DzPzH₂] solutions (not shown here). The extent of the OL effect exhibited by [Ph₈DzPzH₂] is comparable with that shown by [Ph₈DzPzZn]; however, a critical survey of the results in terms of the ISC rate might be inappropriate because of (a) the possible occurrence of a basically different mechanism of nonlinear absorption in [Ph₈DzPzH₂] involving the sequence of the transitions [0 → 1] and [1 → 2]³⁷ and (b) the absence of the LMCT process associated with the absorption of the excited triplet state [3 → 4] (Figure 5).⁴⁴

It is noteworthy to point out that the level of OL effectiveness exhibited by the investigated [Ph₈DzPzM] species is below that of the analogous metallophthalocyanines,^{13,47} metallonaphthalocyanines,⁴⁸ or metallotetraporphyrins.⁴⁹ This can be ascribed to the noncoplanar arrangement of the peripheral diazepine rings with the central porphyrazine core (Figure 1) and the consequent lack of contribution to the π-electron conjugation.⁵⁰ Under these conditions, a concomitant decrease of the electronic polarizability in these structures is expected with respect to more extensively π-conjugated macrocycles.⁵¹ Such a decrease is generally accompanied by a less efficient OL effect due to the direct proportionality that exists between

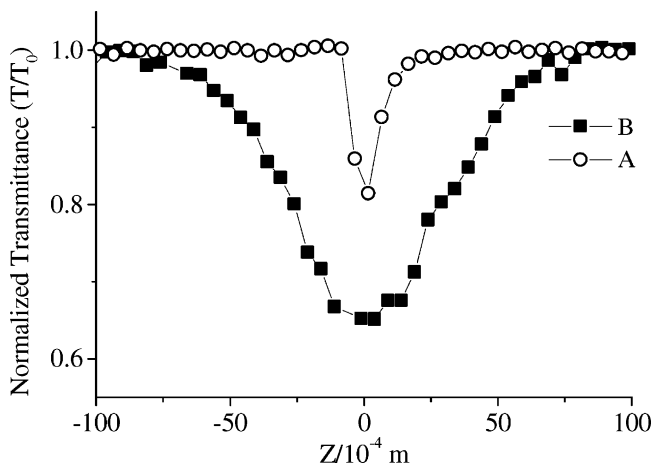


Figure 7. Z-scan profiles of [Ph₈DzPzMn] in toluene solution; T₀ = 92% (A) and 63% (B). Curve A refers to the more diluted solution (C = 3.6 × 10⁻⁵ M), curve B to a saturated solution (C = 1 × 10⁻³ M).

the nonlinear absorption coefficient responsible for the OL effect and the third-order term of the electronic polarizability.⁵²

It is generally observed that the OL effect generated by a species in solution varies with its concentration.⁵³ This is probably due to the fact that the nature of the photophysically active species changes with concentration. Upon moving from dilute to concentrated solutions, the new array of molecular units eventually formed might have electronic states with relative lifetimes considerably different from those of the single molecular unit. In Figure 7 the behavior of the manganese complex [Ph₈DzPzMn] is shown as an example. The increase in concentration of the complex from 3.5 × 10⁻⁵ M (curve A) to about 1 × 10⁻³ M (curve B), accompanied by the concomitant decrease of the linear transmittance, causes an enlargement of the range of light intensity values at which nonlinear absorption occurs. Moreover, a larger decrease of the normalized transmittance

(47) (a) Rao, D. N.; Blanco, E.; Rao, S. V.; Aranda, F. J.; Rao, D. V. G. L. N.; Tripathy, S.; Akkara, J. A. *J. Sci. Ind. Res.* **1998**, *57*, 664. (b) Cooper, T. M.; Campbell, A. L.; Su, W.; Obermeier, K.; Natarajan, K.; Crane, R. L.; Adams, W. W.; Brant, M. *Mater. Res. Soc. Symp. Proc.* **1995** (volume date 1994), *374*, 99. (c) Kohlman, R.; Klimov, V.; Shi, X.; Grigorova, M.; Mattes, B. R.; McBranch, D.; Wang, H.; Wudl, F.; Noguez, J. L.; Moreshead, W. *Mater. Res. Soc. Symp. Proc.* **1998**, *488*, 237. (d) Li, C.; Zhang, L.; Yang, M.; Wang, H.; Wang, Y. *Phys. Rev. A* **1994**, *49*, 1149.

(48) Song, Y.; Wang, Y.; Li, J.; Fang, G.; Yang, X.; Wu, Y.; Liu, Y.; Zuo, X.; Zhu, Q.; Chen, N. *SPIE Proc.* **1998**, *3554*, 241.

(49) (a) Stiel, H.; Volkmer, A.; Ruckmann, I.; Zeug, A.; Ehrenberg, B.; Roder, B. *Opt. Commun.* **1998**, *155*, 135. (b) Hagan, D. J.; Miesak, E.; Negres, R.; Ross, S.; Lim, J.; Van Stryland, E. W.; Dogariu, A. *SPIE Proc.* **1998**, *3472*, 80.

(50) Garratt, P. J. *Aromaticity*; McGraw-Hill: Maidenhead, U.K., 1971.

(51) Nalwa, H. S.; Hanack, M.; Pawlowski, G.; Engel, M. K. *Chem. Phys.* **1999**, *245*, 17.

(52) (a) Boyd, R. W. *Nonlinear Optics*; Academic Press: New York, 1991. (b) Gubler, U.; Bosshard, C. In *Polymers for Photonics Applications I*; Advances in Polymer Science; Lee, K. S., Ed.; Springer: Berlin, 2002; Vol. 158, pp 123–191. (c) Prior, Y.; Vogt, H. *Phys. Rev. B* **1979**, *19*, 5388.

(53) (a) Riggs, J. E.; Sun, Y. P. *J. Chem. Phys.* **2000**, *112*, 4221. (b) Couris, S.; Koudoumas, E.; Ruth, A. A.; Leach, S. *J. Phys. B* **1995**, *28*, 4537.

Table 2. Half-Wave Potentials^a of [Ph₈DzPzZn] in CH₂Cl₂ or Pyridine Containing 0.1 M TBAP

M	solvent	oxidation		reduction				
		<i>E</i> _{pa}	<i>E</i> _{pc}	<i>E</i> ₁	<i>E</i> ₂	<i>E</i> ₃	<i>E</i> ₄	<i>E</i> ₅
Zn ^{II}	CH ₂ Cl ₂	1.03	0.65	-0.73	-0.94	-1.23	-1.51	-1.68 ^b
	pyridine	0.96	0.64	-0.72	-1.04	-1.33	-1.49	-1.72 ^c
Cu ^{II}	pyridine		0.76	-0.56	-0.79	-1.10 ^c	-1.30 ^c	-1.48 ^{c,d}
	2H	CH ₂ Cl ₂		-0.42	-0.66	-1.02 ^c	-1.15 ^c	-1.34 ^c
Co ^{II}	CH ₂ Cl ₂	1.11	0.66	-0.24 ^c	-0.58	-0.97	-1.50	
	pyridine	1.10 ^c	0.64	-0.49	-0.73	-1.05	-1.40	-1.68
Mn ^{II}	pyridine		-0.20 ^c	-0.52	-0.88	-1.22	-1.51	
	CH ₂ Cl ₂ ^f	1.35	-0.05	-0.35	-0.72	-1.00	-1.16 ^g	

^a Half-wave potentials are given in volts vs saturated calomel electrode (SCE). ^b Further reductions can be observed at *E*_{pc} = -1.92 V. ^c *E*_{pc}, scan rate at 0.1 V/s. ^d Further reductions can also be observed at *E*_{pc} = -1.64 and *E*_{1/2} = -1.76 V. ^e *E*_{pa}, scan rate at 0.1 V/s. ^f Upon dissolution in CH₂Cl₂, the initial Mn^{II} complex is oxidized to its Mn^{III} form. ^g Further reductions can also be observed at *E*_{pc} = -1.42, -1.60, and -1.80 V.

tance is observed at the point of maximum irradiation (*Z* = 0). Such results have important practical implications, because they show that a compromise must be reached between high linear transmittance and a strong OL effect if the active system of a limiting optical device is a molecular nonlinear absorber.^{11–13}

Electrochemical Measurements. Electrochemical and spectroelectrochemical measurements on the investigated diazepinoporphyrazine macrocycles were carried out in CH₂Cl₂ and pyridine containing 0.1 (CV) or 0.2 M TBAP (spectroelectrochemistry), and the resulting data (Table 2) will be discussed for the [Ph₈DzPzZn] complexes in the following sequence: M = Zn^{II}, Cu^{II}, 2H, Co^{II}, and Mn^{II}.

Zn^{II}. Data on this complex were obtained in both CH₂Cl₂ and pyridine. The cyclic voltammetric behavior of the Zn^{II} complex upon oxidation in CH₂Cl₂ is illustrated in Figure 8 (see Figure S2 for cyclic voltammograms in pyridine). Two reversible oxidations are seen in CH₂Cl₂ (Figure 8, top panel), and because Zn^{II} is redox-inactive, both processes must involve the macrocyclic ligand. The spectroelectrochemical changes observed upon the first oxidation in both CH₂Cl₂ and pyridine are quite similar to each other. They are shown in Figure 8, top panel, for the CH₂Cl₂ solution and consist of (a) the complete disappearance of the *n* → *π** absorption initially located at 673 nm and earlier mentioned as specifically related to the 6H tautomeric formulation [Ph₈(6HDz)PzZn] (**I**, Chart 1) for the macrocycle, (b) the appearance of a new *Q* band, bathochromically shifted from 634 to 668 nm, and (c) minor changes in the residual UV–vis region explored. The final spectrum of the singly oxidized Zn^{II} complex possesses single Soret and *Q* bands and closely resembles spectra normally observed for neutral symmetric metalloporphyrines.¹⁷ It differs, however, from what is expected for porphyrazine-centered *π*-cation radicals, e.g., for the singly oxidized Mg^{II} and Zn^{II} phthalocyanines,⁵⁴ which show specific UV–vis absorptions of low intensity in the 400–550 nm window and above 700 nm, along with an almost complete absence of intense Soret and *Q* bands. Clearly, then, the first oxidation of [Ph₈DzPzZn] does not take place on the metal center or on the internal porphyrine core. Rather, electron abstraction seems to occur at the peripheral diazepine rings, thus producing form **IV** of the compound (Chart 1), in keeping with similar formulations of stable +1 charged quasi-aromatic simple diazepinium salts.^{55,56}

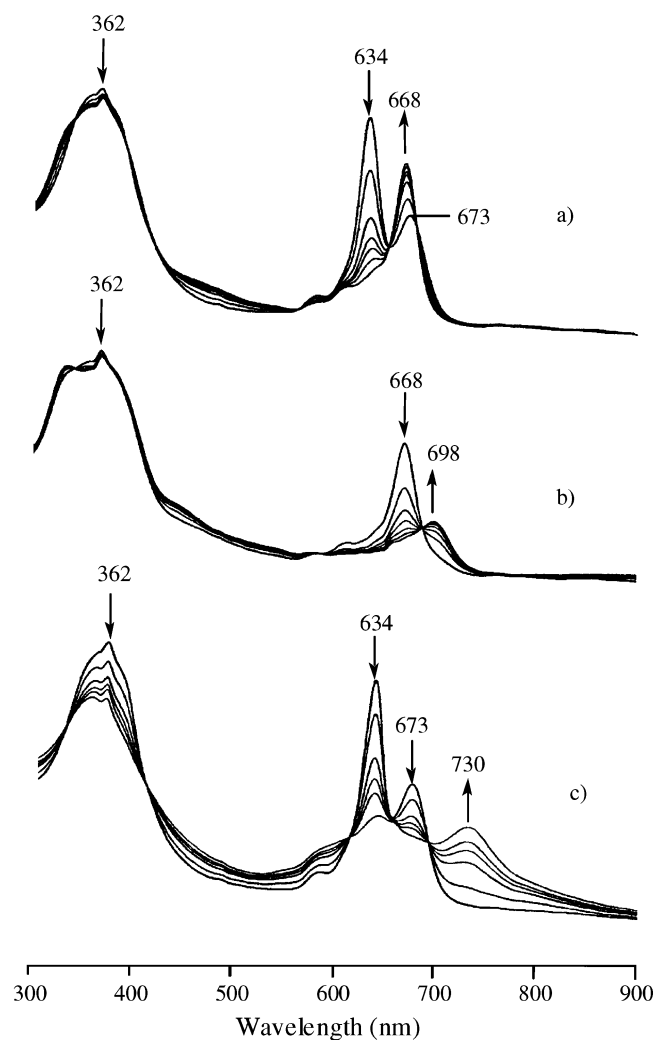
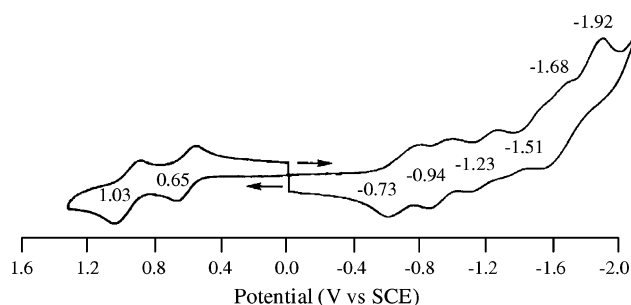


Figure 8. Electrochemical properties of [Ph₈DzPzZn] in CH₂Cl₂: cyclic voltammogram at 0.1 M TBAP and UV–visible spectral changes obtained during controlled potentials electrolysis at 0.2 M TBAP and (a) +0.80 V (first oxidation), (b) +1.20 V (second oxidation), and (c) -0.85 V (first reduction).

The second reversible one-electron oxidation of [Ph₈DzPzZn] leads to formation of an overall +2 charged Zn^{II} complex. The spectral changes accompanying this oxidation are shown in Figure 8b and consist of a *Q*-band bathochromic shift from 668 to 698 nm. Once again, a valid assumption is that the second oxidation does not take place on the internal porphyrine core and is pushed externally to the diazepine rings. The suggested doubly charged oxidized species formulated as [Ph₈(1HDz)-

(54) Stillman, M. J. In *Phthalocyanines—Properties and Applications*; Leznoff, C. C., Lever, A. B. P., Eds.; VCH Publishers: New York, 1993; Vol. 3, pp 227–296.

(55) Lloyd, D.; McNab, H. *Adv. Heterocyclic Chem.* **1998**, *71*, 1–56.

(56) Sharp, J. T. In *Comprehensive Heterocyclic Chemistry*; Katritzky, A. R., Rees, C. W., Eds.; Pergamon Press: Oxford, U.K., 1984; Vol. 7, Part 5, Lwowski, W., Ed., pp 593–651.

PzZn^{2+} (V, Chart 1) shares similarities with the tetraprotonated non-oxidized form produced in 96% H_2SO_4 solution and discussed before.⁷

Although the first oxidation potentials of the Zn^{II} -diazepino-porphyrazine complex and $[\text{PcZn}]$ or its tetra-*t*-butyl derivative $[\text{tBu}_4\text{PcZn}]$ are practically identical,⁵⁷ the second oxidation of $[\text{Ph}_8\text{DzPzZn}]$ is located at a half wave potential that is about 300 mV less positive than $E_{1/2}$ for oxidation of $[\text{tBuPcZn}]$, i.e. it is more easily oxidized. This is consistent with the suggested peripheral localization of the first positive charge in the monocation, which evidently makes a further oxidation more favorable as compared to the case of the phthalocyanine analogues, for which the second oxidation step must occur at an already positively charged highly conjugated macrocycle.

Cyclic voltammograms of the Zn^{II} complex in CH_2Cl_2 and pyridine show several reductions (Table 2, Figure 8, and Figure S2 of Supporting Information). The first two processes are well-defined and fully reversible. The potential of the first reduction is not solvent-dependent (-0.73 and -0.72 V vs SCE in CH_2Cl_2 and pyridine, respectively), while the second reduction is slightly favored in CH_2Cl_2 (-0.94 V vs SCE; -1.04 V in pyridine). The spectral changes that accompany the first reduction are similar in the two solvents and an example of the spectroelectrochemical data is shown in Figure 8c for reduction in CH_2Cl_2 . As seen in this figure, the intensity of the Soret and especially of the Q band is decreased upon reduction and the Q_n band, still present, undergoes a significant bathochromic shift from 673 to 730 nm in CH_2Cl_2 (from 677 to 747 nm in pyridine). Moreover, weak shoulders are detectable at long wavelengths (>800 nm). The similarity of the spectral changes to what is observed upon formation of the singly reduced Mg^{II} and Zn^{II} phthalocyanine complexes, i.e., $[\text{Pc}(-3)\text{Mg}]$ ⁵⁸ and $[\text{Pc}(-3)\text{Zn}]$,⁵⁹ seems to suggest that reduction takes place at the inner porphyrazine site, the annulated diazepine rings retaining their 6*H* tautomeric form. The first reduction product in this case can then be assigned the formula $[\text{Ph}_8(6\text{HDz})\text{Pz}(-3)\text{Zn}]$. Similar half-wave potentials are obtained for the first reduction of $[\text{PcMg}]$ (-0.91 V vs SCE in DMF)⁶⁰ and $[\text{PcZn}]$ (-0.86 V vs SCE in DMF).⁶¹ The reductions of $[\text{Ph}_8\text{DzPzZn}]$ all occur at less negative potentials than for $[\text{PcZn}]$,^{57,62} the differences in the corresponding half-wave potentials becoming progressively more marked (ca. 140 mV vs SCE for first reduction and 260, 520, and 760 mV vs SCE for the second, third, and fourth processes, respectively). Indeed, two additional reduction processes are also observed at more negative potentials in the case of $[\text{Ph}_8\text{DzPzZn}]$ (see Figure 8). It is believed that the stepwise reduction of $[\text{Ph}_8\text{DzPzZn}]$ is greatly facilitated by a delocalization of the negative charges on the peripheral diazepine rings, which, through 6*H*–1*H* tautomerism, are certainly capable of increasing peripheral charge transfer and redistribution. It is noteworthy that simple species containing a 1,4-diazepine ring—

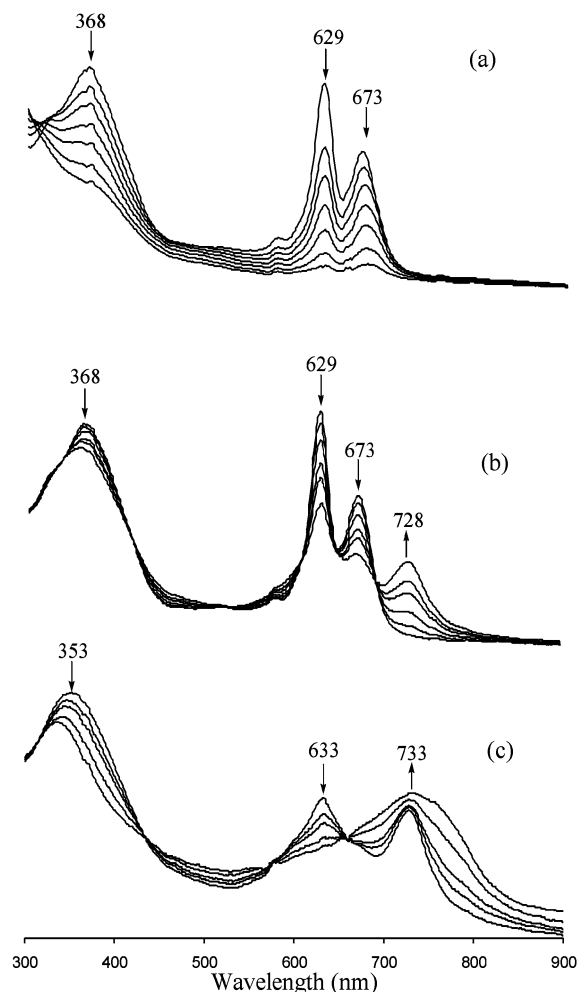


Figure 9. UV–visible spectral changes obtained during controlled potential electrolysis of $[\text{Ph}_8\text{DzPzCu}]$ at (a) $+0.90$ V (first oxidation), (b) -0.60 V (first reduction), and (c) -0.85 V (second reduction), in pyridine containing 0.2 M TBAP.

the initial dinitrile precursor 5,7-diphenyl-3,4-dicyano-1,4-diazepine ($\text{Ph}_2\text{Dz}(\text{CN})_2$) and the benzoannulated analogue 2,4-diphenyl-1,5-3*H*-benzodiazepine (Ph_2DzBz)—both undergo reductions involving heterocyclic or benzene moieties at more negative potentials (-1.03 and -1.96 V vs SCE, respectively; see Text S2 and Figure S1 in Supporting Information) than the macrocyclic species $[\text{Ph}_8\text{DzPzZn}]$.

Cu^{II} . Cyclic voltammograms were obtained for $[\text{Ph}_8\text{DzPzCu}]$ in pyridine. An attempted exploration revealed that a complicated behavior is shown by the complex in CH_2Cl_2 due to the prevalent irreversible processes observed in this solvent at negative potentials. The data in pyridine (Table 2) show only one oxidation at $E_{1/2} = +0.76$ V vs SCE, which is 120 mV more positive than the half-wave potential for the first oxidation of the corresponding Zn^{II} complex. The oxidation of $[\text{Ph}_8\text{DzPzCu}]$ is accompanied by a concomitant precipitation of the electrogenerated species, as clearly indicated by the associated UV–vis spectra, which show a progressive decrease of all absorption bands during the redox process (Figure 9a). This precipitation of the singly oxidized Cu^{II} species is very likely the result of some type of dimerization and/or oligomerization of the electrogenerated π -cation radical and has also been observed for related phthalocyanine and porphyrazine radical species.⁵⁴ The different behavior shown by the Zn^{II} complex,

(57) Lever, A. B. P.; Milaeva, E. R.; Speier, G. In *Phthalocyanines—Properties and Applications*; Leznoff, C. C., Lever, A. B. P., Eds.; VCH Publishers: New York, 1993; Vol. 3, pp 1–69.

(58) Mack, R.; Kirkby, S.; Ough, E.; Stillman, M. J. *Inorg. Chem.* **1992**, *31*, 1717.

(59) Clack, D. W.; Yandle, J. R. *Inorg. Chem.* **1992**, *11*, 1738.

(60) Clack, D. W.; Hush, N. S.; Woosley, I. S. *Inorg. Chim. Acta* **1976**, *19*, 129.

(61) Giraudeau, A.; Louati, A.; Gross, M.; Andre, J. J.; Simon, J.; Su, C. H.; Kadish, K. M. *J. Am. Chem. Soc.* **1983**, *105*, 2917.

(62) L'Her, M.; Pondaven, A. In *The Porphyrin Handbook*; Kadish, K. M., Smith, K. M., Guillard, R., Eds.; Academic Press: New York, 2003; Vol. 16, pp 117–170.

i.e., an apparent lack of molecular association and consequent precipitation, may be related to the occurrence of axial coordination of the radical by pyridine or water or to an edge-to-face association process, as reported for a number of Zn^{II} macrocyclic analogues.^{63,64}

The UV–vis spectral evolution associated with the first reversible reduction of the Cu^{II} complex ($E_{1/2} = -0.56$ V vs SCE; Table 2, Figure 9b) parallels what is seen for the corresponding reduction of the Zn^{II} analogue (Figure 8c). The maintenance of the $n \rightarrow \pi^*$ transition, although significantly shifted ($673 \rightarrow 728$ nm), and the marked decrease of the Q band seem to indicate that the first reduction of the Cu^{II} complex is also localized on the porphyrazine system, the $6H$ tautomeric form being retained, i.e., $[Ph_8(6HDz)Pz(-3)Cu]$. The second reduction of $[Ph_8DzPzCu]$ is a well-defined reversible process occurring at $E_{1/2} = -0.79$ V vs SCE. Several other reduction processes can also be seen at more negative potentials, but these are not well-defined, and upon the reverse scan (oxidation), an irreversibility of the second reduction step is observed. The acceptance of an electron by the macrocyclic framework of the Cu^{II} complex is thermodynamically favored ($E_{1/2} = -0.56$ V in pyridine) compared to the phthalocyanine analogue $[PcCu]$, for which the first reduction (-0.84 V vs SCE) occurs at a more negative potential⁵⁷ than the second reduction of the diazepinoporphyrazine complex.

The spectral changes that accompany the second reduction of $[Ph_8DzPzCu]$ (Figure 9c) give a clear indication that the diazepine rings are directly involved in the acceptance of the negative charge of the reduced species, thus further supporting a hypothesis already advanced for the second reduction of the Zn^{II} analogue. In fact, the final spectrum of the doubly reduced Cu^{II} complex shows no absorptions that would be expected to be seen in the 400–550 nm region for a porphyrazine dianionic species, as is found for the case of $[Pc(-4)Mg]$ (which has an intense absorption at 508 nm).⁵⁴

Free-Base $[Ph_8DzPzH_2]$. No anodic processes, and hence no oxidation reactions, are observed for this species in CH_2Cl_2 but two well-resolved reductions are observed in this solvent at $E_{1/2} = -0.42$ and -0.66 V vs SCE. There are also other less well-defined redox processes that occur at more negative potentials. The first two reductions of free-base $[Ph_8DzPzH_2]$ are located at markedly less negative potentials than for the tetra-*t*-butyl-phthalocyanine analogue, $[tBu_4PcH_2]$ (in CH_2Cl_2 , $E_{1/2} = -0.82$ and -1.19 V vs SCE⁵⁷) and this indicates a strong participation of the diazepine rings in stabilization of the macrocyclic anionic forms.

Co^{II} . Very similar half-wave potentials for oxidation of $[Ph_8DzPzCo]$ were measured in CH_2Cl_2 and in pyridine [see Table 2 and Figure 10 (top) for the cyclic voltammogram in CH_2Cl_2]. As to the first oxidation, this can be compared to the data and assignments for the Co^{II} phthalocyanine^{57,62} and porphyrin⁶⁵ systems, for which values of potential and site of oxidation are both strongly solvent-dependent. In a noncoordinating solvent,

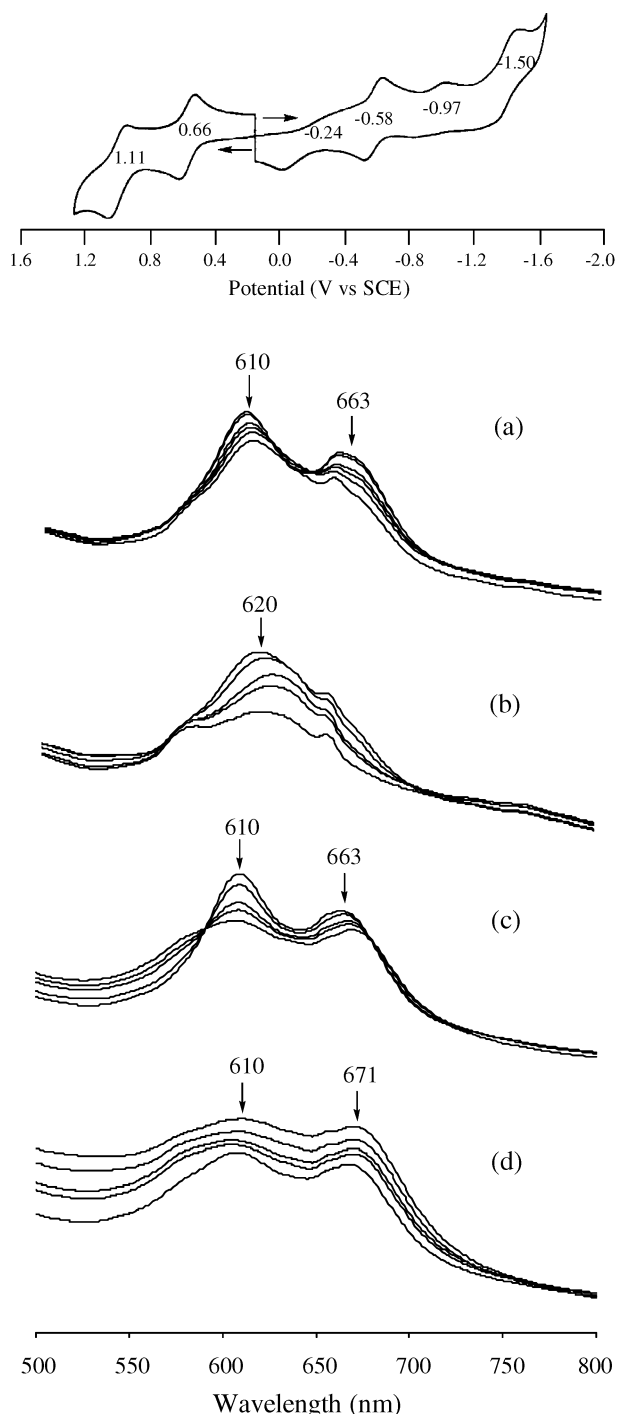


Figure 10. Electrochemical properties of $[Ph_8DzPzCo]$ in CH_2Cl_2 : cyclic voltammogram in solutions of 0.1 M TBAP and UV–visible spectral changes obtained during controlled potentials electrolysis at 0.2 M TBAP and (a) +0.80 V, (b) +1.20 V, (c) -0.40 V, and (d) -0.80 V.

the first oxidation of $[PcCo]$ (dichlorobenzene $E_{1/2} = +0.61$ V vs SCE⁵⁷) is assigned as ligand-centered. For $[TPPCo]$, the oxidation is often assumed as metal-centered, but a ring-centered oxidation has been observed in dry noncoordinating solvents containing weakly coordinating anions.⁶⁵ In coordinating solvents, axial ligation at the metal center stabilizes Co^{III} and hence the oxidation of $[PcCo]$ ⁵⁷ and $[TPPCo]$ ⁶⁵ is metal-centered and occurs at markedly lower potentials than in noncoordinating solvents. The thin-layer spectra of $[Ph_8DzPzCo]$ observed during oxidation (Figure 10a) show only slight changes in peak intensity

(63) Buchler, J. W.; Ng, D. K. P. In *The Porphyrin Handbook*; Kadish, K. M., Smith, K. M., Guillard, R., Eds.; Academic Press: New York, 2000; Vol. 3, pp 245–294.

(64) Cook, M. J.; Jafari-Fini, A. *J. Mater. Chem.* **1997**, *7*, 2327.

(65) (a) Kadish, K. M.; van Caemelbecke, E.; Royal, G. In *The Porphyrin Handbook*; Kadish, K. M., Smith, K. M., Guillard, R., Eds.; Academic Press: New York, 2000; Vol. 8, pp 1–114. (b) Kadish, K. M.; Royal, G.; van Caemelbecke, E.; Gueletti, L. In *The Porphyrin Handbook*; Kadish, K. M., Smith, K. M., Guillard, R., Eds.; Academic Press: New York, 2000; Vol. 9, pp 1–219.

and small shifts of the Q and Q_n bands. This spectral behavior markedly differs from what is expected for π -cation radical formation (and observed for the Zn^{II} and Cu^{II} analogues) and this favors a metal-centered $Co^{II} \rightarrow Co^{III}$ process. The high value of the potential measured for this process points out to the strong electron-withdrawing effect of the $-N=C-$ groups in the $6H$ tautomeric form of the diazepine rings, which makes more difficult the oxidation of the macrocycle, concomitantly causing some stabilization of Co^{II} with respect to Co^{III} .

As to the second oxidation (+1.11 V vs SCE), a Co^{III}/Co^{IV} process is reasonably excluded and a ligand-centered oxidation of the Co^{III} complex is assumed to occur. The UV-vis spectral changes during the second oxidation (Figure 10b) mainly consist of a decrease of intensity of the Q band, but no information is available as to whether the positive charge is preferentially localized on the central porphyrazine core or more peripherally.

Several ill-defined processes are present for reduction of $[Ph_8DzPzCo]$ in CH_2Cl_2 [see Figure 10 (top)]. The first and third reductions are irreversible and appear to involve coupled chemical reactions. The first electroreduction is assigned as the Co^{II}/Co^I process on the basis of results in the literature for $[PcCo]^{57}$ and $[TPPCo]^{65}$ and UV-visible spectra obtained in this study during the spectroelectrochemical reduction of $[Ph_8DzPzCo]$ in a thin-layer cell. The observed spectral evolution during the first reduction of the complex indicates that the two Q and Q_n bands in the 600–700 nm region are maintained (Figure 10c), which means that the effect of the metal reduction on the macrocycle displaying peripherally the tautomeric form $6H$ is small.

Additional well-defined reductions of $[Ph_8DzPzCo]$ are seen at -0.58 and -1.50 V vs SCE, and these half-wave potentials are close to values observed for the reduction of $[PcCo]$ in nondonor solvents.⁵⁷ The spectral changes obtained during the second reduction at -0.80 V are shown in Figure 10d and suggest a ring-centered process. However, it should be noted that the shapes of the current-voltage curves in CH_2Cl_2 depended upon the scan rate, suggesting ligand-exchange processes accompanying electron transfer and possibly reaction of the electrogenerated compounds with the solvent on longer time scales. The redox processes are better defined in pyridine and care must be taken when the data are analyzed in CH_2Cl_2 , since this solvent and other chlorinated hydrocarbons are known to react with reduced Co^{II} macrocycles such as $[TPPCo]$. Thus, some of the less well-defined reduction processes in CH_2Cl_2 may be due to electron transfers involving new products formed in side reactions with the solvent.

Mn^{II}. Fairly well-defined cyclic voltammetric behavior is obtained for $[Ph_8DzPzMn]$ in pyridine (Figure 11) or CH_2Cl_2 . The Mn^{II}/Mn^{III} process is quasi-reversible in both solvents (slow electron transfer) and occurs at -0.05 V (CH_2Cl_2) or -0.20 V (py). The process is listed as an oxidation of Mn^{II} in Table 2 but some Mn^{III} is formed under the electrochemical conditions and a reduction thus appears to be observed upon sweeping the potential in a negative direction from $+0.2$ V vs SCE. Four well-defined one-electron reduction processes are obtained for the Mn^{II} complex $[Ph_8DzPzMn]$ in pyridine (see Figure 11 and Table 2), and these occur at half-wave potentials of -0.52 , -0.88 , -1.22 , and -1.51 V vs SCE. These are all accounted for by assuming a stepwise reduction at the macrocycle. In contrast to the rich reductive redox behavior of this macrocycle,

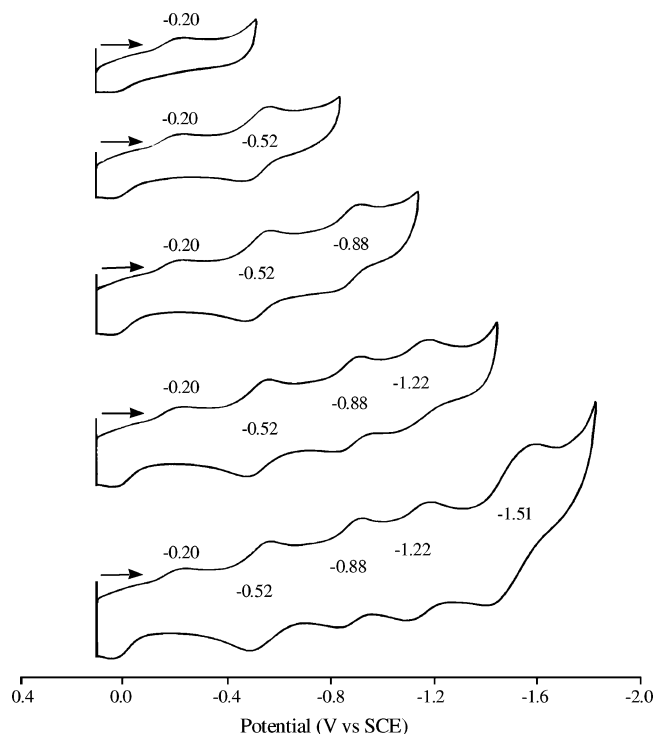


Figure 11. Cyclic voltammograms of $[Ph_8DzPzMn]$ in pyridine containing 0.1 M TBAP.

$[PcMn]$ shows only one reduction at -0.79 V in pyridine and two reductions at -0.69 and -1.46 V vs SCE in DMF.^{57,62} Thus, in the case of $[Ph_8DzPzMn]$ the direct involvement and contribution of the diazepine rings to the multistep reduction behavior appear to be evident.

Conclusions

Further information has been obtained on a new class of tetrapyrrolic macrocycles carrying peripherally annulated seven-membered rings, i.e., tetrakis-2,3-(5,7-diphenyl-6H-diazepino)-porphyrazine, $[Ph_8DzPzH_2]$, and their metal derivatives, $[Ph_8DzPzM]$. We have described new synthetic procedures and new metal complexes, featuring promising developments for the preparation of new tailored metal derivatives. The UV-visible solution spectra of these compounds in different media (basic, neutral, and acidic) confirm previous findings⁷ on the multifaceted participation of the external diazepine rings, through tautomeric and protonated forms, to electron sharing within the entire metal-macrocycle framework. Nonlinear optical investigations, namely, optical limiting measurements, have shown that the $[Ph_8DzPzM]$ complexes behave in solution like reverse-saturable absorbers (RSA), which show reduced transmittance with increase of irradiation. Such nonlinear optical features have been examined by using the generalized five-level model describing the mechanism of the process of sequential two-photon absorption occurring at high levels of irradiation. It was observed that $[Ph_8DzPzZn]$ and $[Ph_8DzPzMn]$ exhibit the strongest optical limiting effect. An explanation for this result seems to come from the high electronic polarizability of the closed d shell for Zn^{II} and the high-spin electronic state for Mn^{II} ; such electronic features would accelerate the intersystem crossing, leading to formation of the highly absorbing state of the two species. It was generally found that the range of irradiation intensity at which solutions of the different $[Ph_8DzPzM]$ species

showed nonlinear optical behavior varied with the concentration of the active species. The electrochemical and spectroelectrochemical behavior, while it clearly substantiates the capacity of the macrocyclic species to undergo multistep redox processes, especially in the region of negative potentials, provides evidence for a direct involvement of the external diazepine rings to electron capture and redistribution with associated stabilization of the various mono- or multicharged species.

Acknowledgment. Thanks are expressed to P. Galli for elemental analyses and useful discussions. Financial support by the MIUR (C.E., 9903263473), the Robert A. Welch Foundation (K.M.K., Grant E-680), a bilateral exchange program (C.E. and P.A.S.) active between the University of "La Sapienza" (Roma) and Ivanovo State University of Chemical Technology (Russia), and an exchange program between the University of Houston and the University of Rome is gratefully acknowledged. Thanks are expressed to W. Blau (Department of Physics at Trinity

College, Dublin, Ireland) for offering the equipment for optical limiting experiments.

Supporting Information Available: Text S1 with detailed description of the synthetic procedures for the precursor and the hydrated macrocyclic complexes $[\text{Ph}_8\text{DzPzM}]$ ($M = \text{Mn}^{\text{II}}$, Co^{II} , Zn^{II} , Cu^{II}) in either pyridine or DMSO; Tables S1 and S2 with UV-vis spectral data in different solvents; text S2 with description of the electrochemical behavior of the precursor 2,3-dicyano-5,7-diphenyl-6*H*-1,4-diazepine, $\text{Ph}_2\text{Dz}(\text{CN})_2$, and two related organic compounds, 2,4-diphenyl-1,5-3*H*-benzodiazepine, Ph_2DzBz , and phthalodinitrile, $\text{Bz}(\text{CN})_2$ (Scheme S1 and Figure S1 included); and Figure S2 showing cyclic voltammograms of $[\text{Ph}_8\text{DzPzZn}]$ in pyridine (print/PDF). This material is available free of charge via the Internet at <http://pubs.acs.org/jacs>.

JA0344361